AD-A192 220 AN ANALYSIS OF THE EFFICIENCY AND DIRECTIVITY OF THE SOUND GENERATED BY A (U) TEXAS UNIV AT AUSTIN APPLIED RESEARCH LABS R J CHANDRASEKHAR ET AL. 13 AUG 87 ARL-TR-87-42 N00014-85-K-0819 F/G 20/1 1/2

UNCLASSIFIED NL

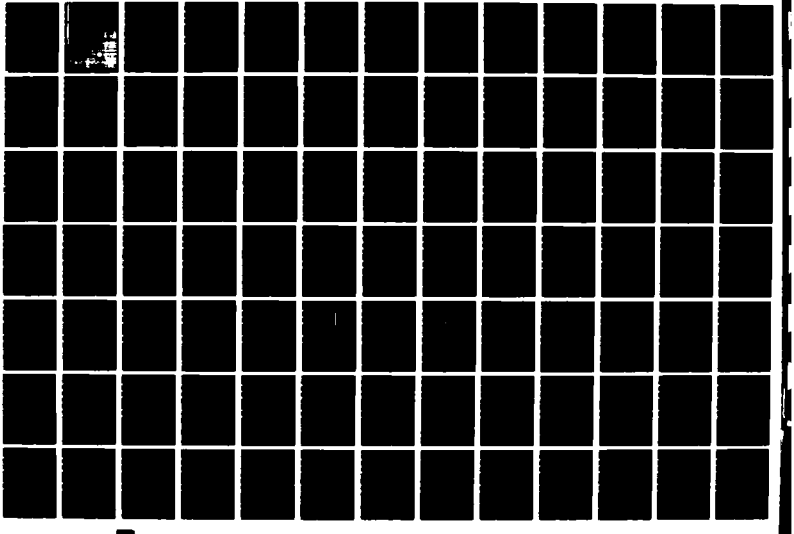

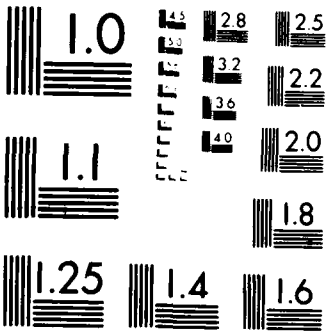
1.0
1.1
1.25
1.4
1.6
1.8
2.0
2.2
2.5
2.8
3.2
3.6
4.0

ARL-TR-87-42 Copy No 22

AN ANALYSIS OF THE EFFICIENCY AND DIRECTIVITY OF THE SOUND GENERATED BY A MOVING LASER SOURCE

FINAL REPORT UNDER CONTRACT N00014-85-K-0819

Rao J. Chandrasekhar
Luis J. Gonzalez
Ilene J. Busch-Vishniac

APPLIED RESEARCH LABORATORIES
THE UNIVERSITY OF TEXAS AT AUSTIN
POST OFFICE BOX 8029, AUSTIN, TEXAS 78713-8029

13 August 1987

Final Report

Approved for public release;
distribution unlimited.

1 September 1985—30 September 1987

Prepared for:

OFFICE OF NAVAL RESEARCH
DEPARTMENT OF THE NAVY
ARLINGTON, VA 22217

UNCLASSIFIED

SECURITY CLASSIFICATION OF THIS PAGE

1193 220

REPORT DOCUMENTATION PAGE

Form Approved OMB No. 0704-0188

1a REPORT SECURITY CLASSIFICATION: UNCLASSIFIED	1b RESTRICTIVE MARKINGS
2a SECURITY CLASSIFICATION AUTHORITY	3 DISTRIBUTION/AVAILABILITY OF REPORT: Approved for public release; distribution unlimited.
2b DECLASSIFICATION/DOWNGRADING SCHEDULE	
4 PERFORMING ORGANIZATION REPORT NUMBER(S): ARL-TR-87-42	5 MONITORING ORGANIZATION REPORT NUMBER(S)
6a NAME OF PERFORMING ORGANIZATION: Applied Research Laboratories; 6b OFFICE SYMBOL (If applicable): ARL:UT	7a NAME OF MONITORING ORGANIZATION: Office of Naval Research
6c ADDRESS (City, State, and ZIP Code): The University of Texas at Austin, P.O. Box 8029, Austin, Texas 78713-8029	7b ADDRESS (City, State, and ZIP Code): Department of the Navy, Arlington, Virginia 22217
8a NAME OF FUNDING/SPONSORING ORGANIZATION; 8b OFFICE SYMBOL (If applicable)	9 PROCUREMENT INSTRUMENT IDENTIFICATION NUMBER: N00014-85-K-0819
8c ADDRESS (City, State, and ZIP Code)	10 SOURCE OF FUNDING NUMBERS: PROGRAM ELEMENT NO; PROJECT NO; TASK NO; WORK UNIT ACCESSION NO

11 TITLE (Include Security Classification): An Analysis of the Efficiency and Directivity of the Sound Generated by a Moving Laser Source

12 PERSONAL AUTHOR(S): Chandrasekhar, Rao J., Gonzalez, Luis J., Busch-Vishniac, Ilene J.

13a TYPE OF REPORT	13b TIME COVERED	14 DATE OF REPORT (Year, Month, Day)	15 PAGE COUNT
final	FROM 85-9-1 TO 87-9-30	87-8-13	121

16 SUPPLEMENTARY NOTATION

17 COSATI CODES		
FIELD	GROUP	SUB-GROUP

18 SUBJECT TERMS (Continue on reverse if necessary and identify by block number): physical acoustics; lasers; underwater sound; thermoacoustics; opto-acoustics

19 ABSTRACT (Continue on reverse if necessary and identify by block number)

In the past decade there has been much work on the sound generated underwater by a moving laser source. In particular, a great deal of effort has been directed toward understanding the thermoacoustic sound generation process, in which the laser heats the fluid medium and radiates sound as a result of the induced volumetric expansion. Theoretical predictions of the laser generated sound and experimental measurements have been shown to agree well for a wide range of source velocities, and source-receiver geometries. The notable exception to this agreement between theory and experiment is for laser beams which are moved at velocities near Mach one. This discrepancy is discussed in Part I of this report.

It was found in earlier experimental studies on moving thermoacoustic sources that transonic motion of the source produces significantly higher sound pressure levels

20 DISTRIBUTION/AVAILABILITY OF ABSTRACT: ☐ UNCLASSIFIED/UNLIMITED ☒ SAME AS RPT ☐ DTIC USERS	21 ABSTRACT SECURITY CLASSIFICATION: UNCLASSIFIED
22a NAME OF RESPONSIBLE INDIVIDUAL: Robert Culbertson	22b TELEPHONE (Include Area Code): (512) 835-3316; 22c OFFICE SYMBOL: ASD

DD Form 1473, JUN 86 — Previous editions are obsolete

SECURITY CLASSIFICATION OF THIS PAGE

UNCLASSIFIED

19. (cont'd)

than predicted by linear theory. This report examines some possible explanations of that observation. In particular, we study the effect of non-linearities in the equation of state due to entropy generation, the variation of sound generating efficiency with time for subsonic and transonic sources, and the validity of linear superposition for a moving thermoacoustic source.

Our analytical study of the effect of a nonlinear equation of state on sound generation for a transonic source shows that such considerations are negligible, being several orders of magnitude smaller than the linear driving term. Numerical results for the efficiency of the sound generating process as a function of time indicate that the efficiency is smaller for a transonic source than for a subsonic source. Hence there is no support for a pumping principle. Finally, experimental work shows that the superposition principle holds better for a transonic source than for either a subsonic or a supersonic source. This surprising result rules out nonlinearities as the cause of the observed boost in sound pressure level for the transonic source.

In Part II of this report we discuss how the sound signal generated by a laser source is affected by various source and receiver parameters. Previously, work on the laser source has been limited to determination of the root mean square sound pressure level as a function of the angle between the receiver and the initial source location. Since the source is moved, the signal received by the hydrophone varies markedly as the source and geometrical parameters of the systems vary. This study determines the relative importance of these parameters. The results could prove to be very useful if the thermoacoustic source is ever employed as an underwater communications device.

In this study a numerical code was used to simulate the acoustic signal observed by a receiver as the source parameters (such as velocity and modulation frequency) and geometrical parameters (such as the initial range and angle between the source and receiver) are varied. Temporal and amplitude signal properties are examined. It is shown that the amplitude properties are, in general, more sensitive to the changes in the system than the temporal properties. Further, it is demonstrated that the source speed and the angle between the source and hydrophone are the most critical parameters.

ACKNOWLEDGMENTS

This research was made possible by a grant from the Office of Naval Research under Contract N00014-85-K-0819 and was performed at Applied Research Laboratories, The University of Texas at Austin. We are thankful to Nicholas Chotiros and Thomas Vittek for their assistance in setting up our experimental apparatus. We are also grateful to Mark Hamilton and David Blackstock for their technical assistance, and to Jim Hawkins, Fred Cotaras, and James TenCate for their assistance in the preparation of this report.

TABLE OF CONTENTS

LIST OF FIGURES

LIST OF SYMBOLS

a	Laser beam radius
A	Coefficient of transmission of light across air-water interface
c	Sound speed in water
C_p	Specific heat of water at constant pressure
C_{p0}	Static value of specific heat of water at constant pressure
f	Laser modulation frequency
h	Depth of receiver
$h(t)$	Impulse response of thermoacoustic source
$I(t)$	Laser intensity
$I_0(t)$	Envelope of laser intensity
I_t	Transmitted light intensity
I_i	Incident light intensity
M	Mach number relative to sound speed in water
N_{DS1}, N_{DS2}	Decimal numbers represented by dipswitches
P	Total pressure
p	Acoustic pressure
p_0	Static pressure
$p_i(t)$	Elementary acoustic pressure
$p_T(t)$	Total acoustic pressure
PPK	Absolute peak pressure of the received signal

$PRMS$	Root means square pressure of the received signal
q	Heat put into the medium per unit volume
r, θ, ϕ	Polar coordinates for a point in the laser heated volume
r_0	Initial range (source to receiver distance)
r_i	Range at an instant i
RM	Initial source Mach number as seen by the receiver, $M \sin\theta_0 \cos\phi_0$
s	Total specific entropy
s_0	Equilibrium specific entropy
δs	Specific entropy causing acoustic disturbance
S	Laser beam cross-section
t	Time coordinate
T	Temperature
T_0	Equilibrium temperature
δT	Temperature change associated with source
$TAVE$	Average of all periods of the received signal
TD	Duration of received signal
$TMAX$	Maximum period of received signal
$TMIN$	Minimum period of received signal
TPK	Time at which the pressure signal peaks
$\mathbf{u}$	Particle velocity
v	Source velocity
$V_{1/2}$	Half-wave voltage of KD*P crystal
V	Voltage applied to Pockels cell
x, y, z	Spatial coordinates
α	Coefficient of absorption of light
β	Coefficient of thermal expansion of water

β_0	Equilibrium value of coefficient of thermal expansion of water
$\delta()$	Dirac delta function
η	Efficiency of the thermoacoustic process
θ_0	Initial angle in the vertical plane between source and receiver
θ_i	Angle in the vertical plane between source and receiver at an instant i
ϑ	Laser irradiated volume
ρ	Total fluid mass density
ρ_0	Equilibrium mass density
$\delta\rho$	Mass density change due to sound
τ_p	Laser pulse duration
ϕ_0	Initial angle in the horizontal plane between source and receiver
ϕ_i	Angle in the horizontal plane between source and receiver at an instant i
ψ	Initial angle between the beam and the vertical axis
ω	Angular frequency of modulation of laser

Part I

SOUND GENERATION BY A TRANSONICALLY MOVING LASER SOURCE

CHAPTER 1

INTRODUCTION

Laser induced sound has been the subject of research around the world for the past 20 years. Much of this work is summarized in two review articles by Lyamshev and Sedov[1] and Lyamshev and Naugol'nykh.[2] There are five mechanisms for the generation of sound by a laser: electrostriction, thermal expansion, surface evaporation, explosive boiling, and optical breakdown. Which of these sound generating processes is dominant depends on the laser and fluid parameters, especially the laser beam energy density. Although the optoacoustic energy conversion efficiency of the mechanism of thermal expansion is relatively low, this is the mechanism that has been primarily investigated because the process is easily controllable, and is capable of producing a highly directional sound source.

In the thermal mechanism, the heating of the medium by a laser causes a temperature rise and a corresponding density drop. Modulation of the laser at frequency f thus generates sound waves at that frequency.

The first substantial work on the generation of sound by heat may be attributed to Ingard[3] who derived a wave equation describing the sound field of a lossless medium containing heat sources. Application of this work to the sound generated by a laser was first described by Westervelt and Larson,[4] who derived the equations which describe the process. Muir, Culbertson, and Clynch[5] later

conducted the first experiments to verify the predictions of Westervelt and Larson. This experimental work was limited to the case where the laser beam is stationary so that heat deposition is confined to a fixed portion of the medium. The energy conversion efficiency for this scheme was found to be quite low, prompting further study into means of enhancing the sound generation efficiency. Bunkin et al.,[6,7] Bozhkov et al.,[8] and Lyamshev and Sedov[9] suggested that a means of increasing the efficiency of sound generation is through the use of a moving thermoacoustic source, in which the laser beam is scanned across a volume of the liquid. They argued that moving the source at Mach 1 could boost the efficiency of the process by causing all of the sound pressures in the direction of motion to add coherently.

Berthelot and Busch-Vishniac[10–12] conducted an extensive analytical and experimental study of moving thermoacoustic sources. Unlike the analyses reported in the Soviet literature, their work is valid for both the nearfield and the farfield, includes the effect of an air-water interface, uses a time domain approach, and includes the effects of a finite beamwidth. Their theoretical model for moving thermoacoustic sources is based on the linear wave equation derived by Larson.[13] Their approach uses numerical predictions based on a convolution-type summation between the impulse response of the system and the thermoacoustic source strength. This theory is well supported by experimental results for the cases of subsonic and supersonic motions of the source. However, a major discrepancy was found for the transonic case where the theoretical model significantly underestimates the measured sound pressure level. Figure (1-1), reproduced from Ref. 12, is typical of the results obtained by Berthelot and Busch-Vishniac. Note that there is roughly a 25 dB disagreement between the predicted and measured results near Mach 1. Based on these results and articles published in Soviet journals[2,14–16] it was suspected that nonlinear effects became

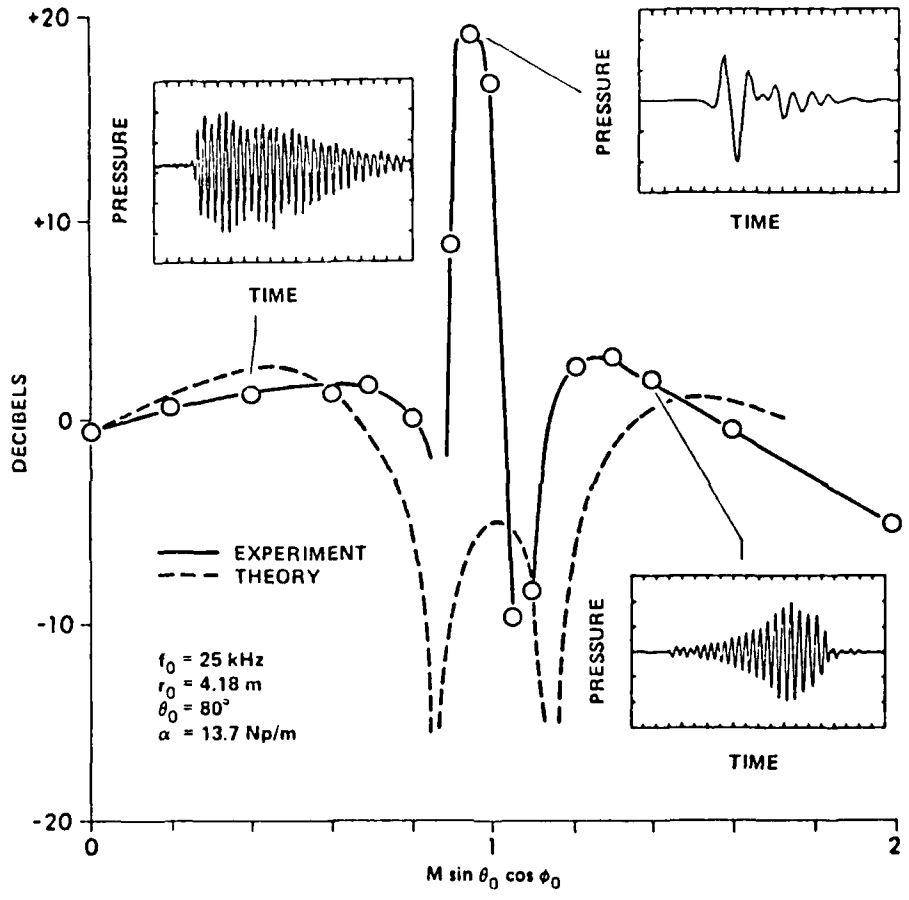

Figure 1-1 Received SPL versus Mach Number of Source

important near Mach 1. In particular, it was suggested that the coefficient of nonlinearity and the specific heat of the medium may both change as the source moves, due to the associated temperature changes.

In recent years, several theories have been proposed for increasing the transduction efficiencies of the thermoacoustic generation of sound. One of them, discussed by Hsieh[17] and Pierce and Hsieh,[18] predicted that the rate of acoustic energy production per unit volume is proportional to the product of the rate of heat addition per unit volume and the local acoustic pressure presently existing at the same point. According to this principle, for maximum efficiency the laser energy deposition scheme should create a traveling acoustic wave and then systematically pump up its amplitude by always adding energy at places where the acoustic pressure has a local maximum.

This report discusses an attempt to determine whether nonlinear interactions may explain the observed discrepancy near Mach 1. The work is partly analytical, partly numerical, and partly experimental. The numerical work is based on the work by Berthelot.[19]

Chapter 2 examines the effect of including fluid properties which vary with temperature through a nonlinear equation of state. A linear, second order wave equation is derived which contains terms to second order in the specific heat and coefficient of thermal expansion of the medium. The effects of these terms in the wave equation are examined theoretically and numerically. Pressure-time waveforms, generated with and without these terms, are compared.

The efficiency of thermoacoustic radiation is the subject of Chapter 3. The expression for efficiency defined by Pierce[20] is evaluated numerically as a function of time for subsonic and transonic motions of the thermoacoustic source on the water surface.

Chapter 4 presents experimental observations designed to determine the importance of nonlinear effects. Verification of the superposition principle is discussed for sources moving at Mach numbers less than, equal to, and greater than one. A detailed description of the experiment and equipment used is also given.

Finally, the results of this part of the study are summarized and relevant conclusions are drawn in Chapter 5.

CHAPTER 2

DERIVATION AND ANALYSIS OF THE LINEAR SECOND ORDER WAVE EQUATION FOR THERMOACOUSTIC SOUND GENERATION

As mentioned earlier, the theoretical model developed by Berthelot and Busch-Vishniac[12] for moving thermoacoustic sources underestimates the measured sound pressure level when the source moves at speeds near Mach 1. Several attempts have been made to explain the discrepancy between theoretical and experimental results for transonic motion of the source on the water surface. One such theory, proposed by Soviet scientists,[2,14-16] put forward the idea that the thermodynamic variables of the medium cannot be taken as invariant. They suggested that the time rate of change of these properties becomes too important to be neglected, especially for source speeds near Mach 1. In particular, concern was expressed regarding the specific heat, C_p, and coefficient of thermal expansion, β.

In this chapter we examine the possible effects of a temperature (and time) varying set of properties of the medium. We develop the partial differential equation describing sound generation in the medium from the standard, linear continuity and conservation of momentum equations, and a nonlinear state equation. The state equation we use includes the normal first order terms plus the second order term which goes as the square of the entropy generated due to the

heat input to the system. All other second order terms in the equation of state are neglected. In this manner we specifically examine only the nonlinear effect attributable to the laser source supplying sufficient heat to cause a change in the properties of the medium. The order of magnitude of each of the resulting second order source terms in the acoustic generation equation is estimated to find those which dominate. The pressure-time response is computed and plotted for each of the predominant source terms, and compared to the first order source term.

2–1 DERIVATION OF THE ENERGY AND WAVE EQUATIONS

Let $P = (p_0 + p)$ be the total pressure in the medium, where p_0 is the static pressure and p is the acoustic pressure generated by the thermal mechanism. Similarly let $\rho = (\rho_0 + \delta\rho)$ be the total density, $T = (T_0 + \delta T)$ the total temperature, and $s = (s_0 + \delta s)$ the total specific entropy of the fluid medium. The terms ρ_0, T_0, and s_0 refer to the equilibrium properties of the medium and $\delta\rho$, δT, and δs are those portions resulting from acoustic disturbances.

The linearized continuity and momentum equations are

$$\rho_t + \rho_0 \nabla \cdot \mathbf{u} = 0 \quad , \tag{2-1.1}$$

$$\rho_0 \mathbf{u}_t + \nabla p = 0 \quad . \tag{2-1.2}$$

Here $\mathbf{u}$ is the particle velocity in the medium and the subscript t denotes a time derivative. For simplicity, it has been assumed that the medium is lossless, nonconvecting, uniform, and irrotational.

In the standard equation of state used in acoustics, one assumes that the density of the medium may be expressed solely in terms of the pressure. For thermally generated sound it is necessary to recognize that the density of the medium is, in general, a function of two independent thermodynamic variables

rather than one. We chose to allow the independent variables to be the specific entropy and pressure. Hence the state equation for this thermal process is

$$\rho = \rho(P, s) \quad . \tag{2-1.3}$$

We use a second order Taylor series expansion to approximate $\delta\rho$ by

$$\delta\rho = \left.\frac{\partial\rho}{\partial P}\right|_0 p + \left.\frac{\partial\rho}{\partial s}\right|_0 \delta s + \frac{1}{2}\left.\frac{\partial^2\rho}{\partial s^2}\right|_0 (\delta s)^2 \quad , \tag{2-1.4}$$

where we have neglected the other second order terms because we assume that variations in s resulting from heating of the medium dominate over variations in p. By definition, the sound speed, c_0, is given by the relation

$$c_0^2 = \left.\frac{\partial P}{\partial\rho}\right|_0 \quad . \tag{2-1.5}$$

Therefore,

$$\left.\frac{\partial\rho}{\partial P}\right|_0 = \frac{1}{c_0^2} \quad . \tag{2-1.6}$$

The coefficient of thermal expansion, β, is defined as

$$\beta = -\frac{1}{\rho}\left.\frac{\partial\rho}{\partial T}\right|_P \quad , \tag{2-1.7}$$

or

$$\beta = -\frac{1}{\rho}\left.\frac{\partial\rho}{\partial s}\right|_P \left.\frac{\partial s}{\partial T}\right|_P \quad . \tag{2-1.8}$$

But, from thermodynamics,

$$\frac{C_p}{T} = \left.\frac{\partial s}{\partial T}\right|_P \quad , \tag{2-1.9}$$

where C_p is the specific heat of the medium. Therefore,

$$\beta = -\frac{1}{\rho}\left.\frac{\partial\rho}{\partial s}\right|_P \frac{C_p}{T} \quad , \tag{2-1.10}$$

and

$$\left.\frac{\partial\rho}{\partial s}\right|_P = -\frac{\rho\beta T}{C_p} \quad . \tag{2-1.11}$$

Differentiating Eq. (2-1.11) with respect to s, we get

$$\left.\frac{\partial^2\rho}{\partial s^2}\right|_0 = -\frac{\rho_0\beta_0 T_0}{C_{p_0}}\left[\frac{1}{T_0}\left.\frac{\partial T}{\partial s}\right|_0 + \frac{1}{\beta_0}\left.\frac{\partial\beta}{\partial s}\right|_0 + \frac{1}{\rho_0}\left.\frac{\partial\rho}{\partial s}\right|_0 - \frac{1}{C_{p_0}}\left.\frac{\partial C_p}{\partial s}\right|_0\right] \quad . \quad (2\text{-}1.12)$$

We may use Eq. (2-1.11) to express $\left.\frac{\partial\rho}{\partial s}\right|_0$ in Eq. (2-1.12), but $\left.\frac{\partial T}{\partial s}\right|_0$, $\left.\frac{\partial\beta}{\partial s}\right|_0$, and $\left.\frac{\partial C_p}{\partial s}\right|_0$ are, as yet, unknown. In general, T, β, and C_p are functions of both P and s. However, since we are assuming that the entropy production dominates over sound generation, and since these coefficients appear in the highest retained order of our approximation for $\delta\rho$, we may approximate T, β, and C_p as functions of s only. Therefore we may write $\left.\frac{\partial\beta}{\partial s}\right|_0 \delta s$ as $\delta\beta$ and similarly define δT and δC_p. Then, our expansion for $\delta\rho$ produces

$$\delta\rho = \frac{p}{c_0^2} + \frac{\rho_0\beta_0 T_0}{2C_{p_0}}\,\delta s\left[-2 - \frac{\delta T}{T_0} - \frac{\delta\beta}{\beta_0} - \frac{\delta\rho}{\rho_0} + \frac{\delta C_p}{C_{p_0}} + \frac{p}{\rho_0 c_0^2}\right] \quad , \quad (2\text{-}1.13)$$

where $\left.\frac{\partial\rho}{\partial s}\right|_0 \delta s$ is approximated to first order as $\delta\rho - \frac{p}{c_0^2}$. Differentiating Eq. (2-1.13) with respect to time yields

$$\begin{aligned}\rho_t \;=\; & \frac{p_t}{c_0^2} + \frac{\rho_0\beta_0 T_0}{2C_{p_0}}\,\delta s\left[\frac{(\delta C_p)_t}{C_{p_0}} - \frac{(\delta T)_t}{T_0} - \frac{(\delta\beta)_t}{\beta_0} - \frac{(\delta\rho)_t}{\rho_0} + \frac{p_t}{\rho_0 c_0^2}\right] \\ & + \frac{\beta_0\rho_0 T_0}{2C_{p_0}}\,s_t\left[\frac{\delta C_p}{C_{p_0}} - 2 - \frac{\delta T}{T_0} - \frac{\delta\beta}{\beta_0} - \frac{\delta\rho}{\rho_0} + \frac{p}{\rho_0 c_0^2}\right] \quad . \quad (2\text{-}1.14)\end{aligned}$$

Eq. (2-1.14) contains terms which explicitly depend upon the time rate of change of entropy produced by the laser heating of the medium. We prefer to express the density perturbation instead in terms of the heat supplied by the laser, so we use the second law of thermodynamics to relate the entropy and heat. Note that this assumes that all of the heat results in an entropy change.

$$s_t = \frac{q}{\rho T} = \frac{q}{(\rho_0 + \delta\rho)}\frac{1}{(T_0 + \delta T)} \quad . \quad (2\text{-}1.15)$$

By taking the binomial expansion of the denominator and retaining the leading terms, we have

$$s_t = \frac{q}{\rho_0 T_0}\left[1 - \frac{\delta T}{T_0} - \frac{\delta\rho}{\rho_0}\right] \quad . \quad (2\text{-}1.16)$$

where q is the heat input per unit volume per unit time. Substituting Eq. (2-1.16) into Eq. (2-1.14) and keeping leading terms, Eq. (2-1.14) simplifies to

$$\rho_t = \frac{p_t}{c_0^2} + \frac{\rho_0 \beta_0 T_0}{2C_{p_0}} \delta s \left[\frac{(\delta C_p)_t}{C_{p_0}} - \frac{(\delta T)_t}{T_0} - \frac{(\delta \beta)_t}{\beta_0} - \frac{(\delta \rho)_t}{\rho_0} + \frac{p_t}{\rho_0 c_0^2} \right] + \frac{\beta_0 q}{2C_{p_0}} \left[\frac{\delta C_p}{C_{p_0}} - 2 + \frac{\delta T}{T_0} - \frac{\delta \beta}{\beta_0} + \frac{\delta \rho}{\rho_0} + \frac{p}{\rho_0 c_0^2} \right] \quad . \tag{2-1.17}$$

Multiplying Eq. (2-1.1) throughout by p, we have

$$p(\nabla \cdot \mathbf{u}) = -\frac{p}{\rho_0} \rho_t \quad . \tag{2-1.18}$$

Taking $\mathbf{u}\cdot$ of Eq. (2-1.2) yields

$$\mathbf{u} \cdot (\rho_0 \mathbf{u}_t) = -\mathbf{u} \cdot \nabla p = -\nabla \cdot (p\mathbf{u}) + p(\nabla \cdot \mathbf{u}) \quad . \tag{2-1.19}$$

Therefore

$$p(\nabla \cdot \mathbf{u}) = \mathbf{u} \cdot (\rho_0 \mathbf{u}_t) + \nabla \cdot (p\mathbf{u}) \quad . \tag{2-1.20}$$

Equating $p(\nabla \cdot \mathbf{u})$ from Eqs. (2-1.18) and (2-1.20),

$$\mathbf{u} \cdot (\rho_0 \mathbf{u}_t) + \nabla \cdot (p\mathbf{u}) = -\frac{p}{\rho_0} \rho_t \quad , \tag{2-1.21}$$

which may be rewritten as

$$\left(\frac{1}{2} \rho_0 \mathbf{u}^2 \right)_t + \nabla \cdot (p\mathbf{u}) = -\frac{p}{\rho_0} \rho_t \quad . \tag{2-1.22}$$

Equation (2-1.22) may be interpreted as an energy equation. The terms on the left hand side are the kinetic and potential energies per unit volume per unit time, and the term on the right hand side is the source factor. Note that since the source term depends upon rho_t, the second order terms in the equation of state have the affect of acting as new source terms.

Substituting for ρ_t from Eq. (2-1.17) in Eq. (2-1.22) yields

$$\left(\frac{1}{2}\rho_0\mathbf{u}^2\right)_t + \nabla\cdot(p\mathbf{u}) + \frac{p}{\rho_0}\frac{p_t}{c_0^2} = \frac{\beta_0 T_0 p}{2C_{p0}}\delta s\left[\frac{T_t}{T_0}+\frac{\beta_t}{\beta_0}+\frac{\rho_t}{\rho_0}-\frac{(C_p)_t}{C_{p0}}-\frac{p_t}{\rho_0 c_0^2}\right] + \frac{\beta_0 pq}{2\rho_0 C_{p0}}\left[2+\frac{\delta\beta}{\beta_0}-\frac{\delta C_p}{C_{p0}}-\frac{\delta T}{T_0}-\frac{\delta\rho}{\rho_0}-\frac{p}{\rho_0 c_0^2}\right] \quad . \qquad (2\text{-}1.23)$$

It is this equation, combined with the conservation of linear momentum and conservation of mass, that will be used to produce a wave equation for the thermoacoustic source. This energy equation is also useful in discussing the efficiency of thermoacoustic generation as will be discussed in the next chapter. For now, it is sufficient to note that the leading order source term in Eq. (2-1.23) goes as the product of q and p, and that all other source terms involve the product of p and other thermodynamic variables.

Consider the energy equation, Eq. (2-1.23). Multiplying throughout by $(-\rho_0/p)$ and regrouping produces

$$-\frac{\rho_0}{p}\mathbf{u}\cdot(\rho_0\mathbf{u}_t+\nabla p)-\rho_0(\nabla\cdot\mathbf{u})-\frac{p_t}{c_0^2} = -\frac{\beta_0 q}{2C_{p0}}\left[2+\frac{\delta\beta}{\beta_0}-\frac{\delta C_p}{C_{p0}}-\frac{\delta T}{T_0}-\frac{\delta\rho}{\rho_0}-\frac{p}{\rho_0 c_0^2}\right] + \frac{\beta_0 T_0\rho_0}{2C_{p0}}\delta s\left[\frac{(C_p)_t}{C_{p0}}-\frac{T_t}{T_0}-\frac{\beta_t}{\beta_0}-\frac{\rho_t}{\rho_0}+\frac{p_t}{\rho_0 c_0^2}\right] \quad . \qquad (2\text{-}1.24)$$

Using the momentum equation, Eq. (2-1.2), Eq. (2-1.24) reduces to

$$-\rho_0(\nabla\cdot\mathbf{u})-\frac{p_t}{c_0^2} = \frac{\beta_0 T_0\rho_0}{2C_{p0}}\delta s\left[\frac{(C_p)_t}{C_{p0}}-\frac{T_t}{T_0}-\frac{\beta_t}{\beta_0}-\frac{\rho_t}{\rho_0}+\frac{p_t}{\rho_0 c_0^2}\right] - \frac{\beta_0 q}{2C_{p0}}\left[2+\frac{\delta\beta}{\beta_0}-\frac{\delta C_p}{C_{p0}}-\frac{\delta T}{T_0}-\frac{\delta\rho}{\rho_0}-\frac{p}{\rho_0 c_0^2}\right] \qquad (2\text{-}1.25)$$

Differentiating this equation with respect to t yields

$$-\rho_0\nabla\cdot\mathbf{u}_t - \frac{p_{tt}}{c_0^2} = \frac{\beta_0 T_0\rho_0}{2C_{p0}}\delta s\left[\frac{(C_p)_{tt}}{C_{p0}}-\frac{T_{tt}}{T_0}-\frac{\beta_{tt}}{\beta_0}-\frac{\rho_{tt}}{\rho_0}+\frac{p_{tt}}{\rho_0 c_0^2}\right]$$

$$+\frac{\beta_0 T_0 \rho_0}{2C_{p_0}} s_t \left[\frac{(C_p)_t}{C_{p_0}} - \frac{T_t}{T_0} - \frac{\beta_t}{\beta_0} - \frac{\rho_t}{\rho_0} + \frac{p_t}{\rho_0 c_0^2}\right]$$
$$-\frac{\beta_0 q_t}{2C_{p_0}} \left[2 + \frac{\delta\beta}{\beta_0} - \frac{\delta C_p}{C_{p_0}} - \frac{\delta T}{T_0} - \frac{\delta\rho}{\rho_0} - \frac{p}{\rho_0 c_0^2}\right]$$
$$-\frac{\beta_0 q}{2C_{p_0}} \left[\frac{\beta_t}{\beta_0} - \frac{(C_p)_t}{C_{p_0}} - \frac{T_t}{T_0} - \frac{\rho_t}{\rho_0} - \frac{p_t}{\rho_0 c_0^2}\right] \quad . \qquad (2\text{-}1.26)$$

Equation (2-1.26) may be reduced using the divergence of the momentum equation (Eq. (2-1.2)) to yield the wave equation including second order terms attributed to time varying thermodynamic parameters:

$$\nabla^2 p - \frac{p_{tt}}{c_0^2} = \frac{\beta_0 T_0 \rho_0}{2C_{p_0}} \delta s \left[\frac{(C_p)_{tt}}{C_{p_0}} - \frac{T_{tt}}{T_0} - \frac{\beta_{tt}}{\beta_0} - \frac{\rho_{tt}}{\rho_0} + \frac{p_{tt}}{\rho_0 c_0^2}\right]$$
$$+\frac{\beta_0 T_0 \rho_0}{2C_{p_0}} s_t \left[\frac{(C_p)_t}{C_{p_0}} - \frac{T_t}{T_0} - \frac{\beta_t}{\beta_0} - \frac{\rho_t}{\rho_0} + \frac{p_t}{\rho_0 c_0^2}\right]$$
$$-\frac{\beta_0 q_t}{2C_{p_0}} \left[2 + \frac{\delta\beta}{\beta_0} - \frac{\delta C_p}{C_{p_0}} - \frac{\delta T}{T_0} - \frac{\delta\rho}{\rho_0} - \frac{p}{\rho_0 c_0^2}\right]$$
$$-\frac{\beta_0 q}{2C_{p_0}} \left[\frac{\beta_t}{\beta_0} - \frac{(C_p)_t}{C_{p_0}} - \frac{T_t}{T_0} - \frac{\rho_t}{\rho_0} - \frac{p_t}{\rho_0 c_0^2}\right] \quad . \qquad (2\text{-}1.27)$$

Note that although the left hand side of this equation contains the standard acoustic terms, there are also pressure dependent terms on the right hand side of Eq. (2-1.27). Note also that there are 20 new terms which appear on the source side of the equation and which result directly from the inclusion of a nonlinear equation of state. The remaining term on the right hand side is the leading order source term which appears in the Westerveld-Larson equation.

The wave equation derived above is too complicated to be analyzed theoretically or numerically. Its complexity can be reduced by making certain simplifying assumptions, and examining the orders of magnitude of some of the source terms. There are two operations which may be readily applied to reduce the complexity of Eq. (2-1.27): eliminating ρ using the equation of state, and expressing all time derivatives of thermodynamic quantities in terms of derivatives

with respect to temperature and time derivatives of temperature.

To eliminate ρ from Eq. (2-1.27), we rewrite $\delta\rho$, ρ_t, and ρ_{tt} using the leading order terms in the state equation. (This is permissible since the terms involving *rho* are all second order.) Making this substitution in Eq. (2-1.27) yields

$$\begin{aligned}\nabla^2 p - \frac{p_{tt}}{c_0^2} = {} & \frac{\beta_0 T_0 \rho_0}{2C_{p0}}\,\delta s\left[\frac{(C_p)_{tt}}{C_{p0}} - \frac{T_{tt}}{T_0} - \frac{\beta_{tt}}{\beta_0} + \frac{\beta_0 q_t}{\rho_0 C_{p0}}\right] \\ & - \frac{\beta_0 q_t}{2C_{p0}}\left[2 + \frac{\delta\beta}{\beta_0} - \frac{\delta C_p}{C_{p0}} - \frac{\delta T}{T_0} - \frac{2p}{\rho_0 c_0^2} + \frac{\beta_0 T_0 \delta s}{C_{p0}}\right] \\ & - \frac{\beta_0 q}{C_{p0}}\left[\frac{\beta_t}{\beta_0} - \frac{(C_p)_t}{C_{p0}} - \frac{p_t}{\rho_0 c_0^2}\right] \quad , \end{aligned} \tag{2-1.28}$$

where we recognize $q = \rho T s_t \approx \rho_0 T_0 s_t$.

If the thermodynamic quantities C_p and β are functions of a single thermodynamic variable, as assumed, then we may express them as $C_p(T)$ and $\beta(T)$. Using the chain rule, then, we may rewrite Eq. (2-1.28) as

$$\begin{aligned}\nabla^2 p - \frac{p_{tt}}{c_0^2} = {} & -\frac{\beta_0 q_t}{2C_{p0}}\left[2 + \frac{\delta\beta}{\beta_0} - \frac{\delta C_p}{C_{p0}} - \frac{\delta T}{T_0} - \frac{2p}{\rho_0 c_0^2}\right] \\ & - \frac{\beta_0 q}{C_{p0}}\left[\frac{T_t \left.\frac{\partial\beta}{\partial T}\right|_{T_0}}{\beta_0} - \frac{T_t \left.\frac{\partial C_p}{\partial T}\right|_{T_0}}{C_{p0}} - \frac{p_t}{\rho_0 c_0^2}\right] \\ & + \frac{\beta_0 T_0 \rho_0}{2C_{p0}}\,\delta s T_{tt}\left[-\frac{1}{T_0} + \frac{\left.\frac{\partial C_p}{\partial T}\right|_{T_0}}{C_{p0}} - \frac{\left.\frac{\partial\beta}{\partial T}\right|_{T_0}}{\beta_0}\right] \quad . \end{aligned} \tag{2-1.29}$$

where we have retained only terms to second order. It is this simplified wave equation which we will examine in order to determine the relative magnitudes of the various source terms.

2–2 MAGNITUDES OF THE SOURCE TERMS IN THE WAVE EQUATION

In order to compare the magnitudes of the source terms appearing in Eq. (2–1.29) it is convenient to relate the perturbations in the thermodynamic variables to q. The expression for q in terms of the intensity (I) of the laser beam has been shown by Larson[13] to be

$$q = -\nabla \cdot \langle I(x,y,z,t) \rangle \quad . \tag{2–2.1}$$

Considering the exponential variation of intensity with depth, z, to be the only spatial variation of intensity within the laser beam, we have

$$q = -\frac{\partial}{\partial z} \left[AI(t) \exp(-\alpha z) \right] S\delta(x - x_c)\delta(y - y_c) \quad , \tag{2–2.2}$$

where A is a constant for a given laser, S is the cross-sectional area of the beam, α is the optical absorption coefficient, and $\delta(x - x_c)$ and $\delta(y - y_c)$ are Dirac delta functions. From the above equation, for a given α and at a given depth,

$$q \propto I(t) \quad . \tag{2–2.3}$$

For the laser used in our research

$$I(t) \propto \frac{t}{\tau_p} \exp(-5(t/\tau_p)) \quad , \tag{2–2.4}$$

where τ_p is the laser pulse duration. Therefore

$$q \propto \frac{t}{\tau_p} \exp(-5(t/\tau_p)) \quad . \tag{2–2.5}$$

The above expressions allow for q and q_t to be expressed in terms of known quantities. However, we may also write q as

$$q = \frac{\partial}{\partial t} (\rho C_p \delta T) \quad . \tag{2–2.6}$$

Equation (2-2.6) may be approximated to leading order by

$$q = \rho_0 C_{p0} T_t \quad , \tag{2-2.7}$$

which may be solved for T_t,

$$T_t = \frac{q}{\rho_0 C_{p0}} \quad . \tag{2-2.8}$$

Integrating this equation with respect to time yields an expression for the temperature rise of a volume caused by the laser heating,

$$\delta T = \frac{1}{\rho_0 C_{p0}} \int q dt \quad . \tag{2-2.9}$$

Hence, we may express T_t and δT in terms of known quantities.

Since C_p and β are assumed to be only functions of T, δC_p and $\delta\beta$ can be expressed as

$$\begin{aligned} \delta C_p &= \left.\frac{\partial C_p}{\partial T}\right|_{T_0} \delta T \\ &= \left.\frac{\partial C_p}{\partial T}\right|_{T_0} \frac{1}{\rho_0 C_{p0}} \int q dt \quad , \end{aligned} \tag{2-2.10}$$

and

$$\begin{aligned} \delta\beta &= \left.\frac{\partial \beta}{\partial T}\right|_{T_0} \delta T \\ &= \left.\frac{\partial \beta}{\partial T}\right|_{T_0} \frac{1}{\rho_0 C_{p0}} \int q dt \quad . \end{aligned} \tag{2-2.11}$$

With these definitions expressions have been obtained for all of the source terms in the simplified wave equation, except for those involving the acoustic pressure. Since Eq. (2-1.29) is linear in pressure, we estimate the strength of the pressure dependent source terms by first determining the pressure response to the leading order source term, and then using this pressure in the second order source terms.

Although this procedure could be iterated to produce a more accurate result, we found that iteration was not necessary.

The wave equation given by Eq. (2-1.29) may be simplified further now by comparing the relative sizes of the source terms. The source terms involving the pressure are ignored in this reasoning since the pressure is an unknown quantity.

In previous studies on thermoacoustic sources, the only source term that was considered was the first order term $-\frac{\beta_0 q_t}{C_{p_0}}$. This, being the only first order term, is indeed the most significant driving term. It was reported in a review article by Lyamshev and Naugol'nykh[2] that the term $-\frac{\beta_t q}{C_{p_0}}$ is the next largest source term. Hence we compare all of the remaining second order terms to this term, in order to justify their inclusion or exclusion in our numerical analysis of the wave equation.

We know that for fresh water at room temperature, $\frac{1}{T_0} \doteq 3.3 \times 10^{-3}$, $\frac{\frac{\partial C_p}{\partial T}\big|_{T_0}}{C_{p0}} \doteq 4.4 \times 10^{-8}$, and $\frac{\frac{\partial \beta}{\partial T}\big|_{T_0}}{\beta_0} \doteq 4.3 \times 10^{-2}$. Therefore the terms involving $\frac{1}{T_0}$ and $\frac{\frac{\partial C_p}{\partial T}\big|_{T_0}}{C_{p0}}$ can be ignored when compared to the one containing $\frac{\frac{\partial \beta}{\partial T}\big|_{T_0}}{\beta_0}$ and the wave equation can be simplified to:

$$\nabla^2 p - \frac{p_{tt}}{c_0^2} = -\frac{\beta_0 q_t}{2C_{p0}}\left[2 + \frac{\delta\beta}{\beta_0} - \frac{\delta C_p}{C_{p0}} - \frac{\delta T}{T_0} - \frac{2p}{\rho_0 c_0^2}\right] - \frac{\beta_0 q}{C_{p0}} T_t \left[\frac{\frac{\partial \beta}{\partial T}\big|_{T_0}}{\beta_0} - \frac{\frac{\partial C_p}{\partial T}\big|_{T_0}}{C_{p0}}\right] - \frac{\beta_0 T_0 \rho_0}{2C_{p0}} \delta s T_{tt} \frac{\frac{\partial \beta}{\partial T}\big|_{T_0}}{\beta_0} + \frac{\beta_0 q p_t}{\rho_0 C_{p0} c_0^2} \quad . \tag{2-2.12}$$

Consider the ratio of the second and sixth terms on the right hand side of Eq. (2-2.12):

$$\text{Ratio 1} = \frac{\delta\beta}{2q} \frac{q_t}{T_t \frac{\partial \beta}{\partial T}\big|_{T_0}} \quad . \tag{2-2.13}$$

Substituting Eqs. (2-2.11) and (2-2.8) for $\delta\beta$ and T_t, we get

$$\text{Ratio 1} = \frac{1}{2q^2}\frac{\partial q}{\partial t}\int q dt \quad , \tag{2-2.14}$$

where the integral is evaluated over the time interval during which a section of the fluid is being heated. Consider a point in the fluid heated by the laser beam. If the beam is assumed to have a circular cross-section, then the point is exposed to heat, at most, for the time it takes for the laser beam to travel a distance equal to the beam diameter. If the diameter of the beam is 2 cm and the laser is moving at Mach 1, (corresponding to our experimental setup) then the section of fluid is heated for a time $t_h = 10^{-5}$ s. Therefore the ratio can be written as

$$\text{Ratio 1} = \frac{1}{2q^2}\frac{\partial q}{\partial t}\int_{t_0}^{t_0+t_h} q dt \quad , \tag{2-2.15}$$

where t_0 varies such that $0 < t_0 < (\tau_p - t_h)$. A computer program has been written to calculate the maximum value of Ratio 1, which was found to be of the order of 0.1. This justifies the elimination of the term $-\frac{\delta\beta}{2C_{p_0}}q_t$ in comparison to the term $-\frac{q}{C_{p_0}}T_t\left.\frac{\partial\beta}{\partial T}\right|_{T_0}$. Note that this conclusion is only valid if the source is moving at approximately Mach 1. If the laser beam is moved more slowly, then t_h and Ratio 1 increase. Since our concern is with an explanation of the discrepancy between theory and experiment observed for a transonic source, we have concentrated on a source moving at Mach 1.

Consider the ratio of the third and seventh terms on the right hand side of Eq. (2-2.12):

$$\text{Ratio 2} = \frac{\delta C_p}{2q}\frac{q_t}{T_t\left.\frac{\partial C_p}{\partial T}\right|_{T_0}} \quad . \tag{2-2.16}$$

Using Eqs. (2-2.10) and (2-2.8), we see that Ratio 2 = Ratio 1. Therefore, by the same analysis used above, the term $\frac{\delta C_p \beta_0 q_t}{2C_{p_0}^2}$ can be neglected when compared to $\frac{\beta_0 q T_t\left.\frac{\partial C_p}{\partial T}\right|_{T_0}}{C_{p_0}^2}$.

Consider the ratio of the seventh and sixth terms on the right hand side of Eq. (2-2.12):

$$\text{Ratio 3} = \frac{\beta_0}{C_{p0}} \frac{\left.\frac{\partial C_p}{\partial T}\right|_{T_0}}{\left.\frac{\partial \beta}{\partial T}\right|_{T_0}} \quad , \tag{2-2.17}$$

which is roughly 1.04×10^{-6} for fresh water at room temperature. Thus it is seen that the seventh term can be neglected in relation to the sixth one.

Estimating the ratio of the fourth and sixth terms on the right hand side of Eq. (2-2.12) for fresh water,

$$\text{Ratio 4} = \frac{\beta_0}{2T_0} \frac{q_t \delta T}{q T_t \left.\frac{\partial \beta}{\partial T}\right|_{T_0}} = \frac{\beta_0}{T_0} \frac{q_t \int q dt}{2q^2 \left.\frac{\partial \beta}{\partial T}\right|_{T_0}} = 8 \times 10^{-3} \quad . \tag{2-2.18}$$

The order of magnitude of Ratio 4 justifies the exclusion of the fourth term.

Consider the ratio of the eighth and sixth terms on the right hand side of Eq. (2-2.12):

$$\text{Ratio 5} = \frac{T_0 \rho_0 \delta s T_{tt}}{2 q T_t} \quad . \tag{2-2.19}$$

We may find an expression for T_{tt} by differentiating Eq. (2-2.8). Since $\delta s = (\int q dt)/(\rho_0 T_0)$, this leads to the conclusion that Ratio 5 and Ratio 1 are the same which supports the exclusion of the eighth term compared to the sixth one. Examining the ratios defined above, it is obvious that the sixth term on the right hand side of Eq. (2-2.12) is indeed the biggest second order term (excluding the possible exception of the pressure dependent terms, which are evaluated iteratively).

2–3 NUMERICAL SOLUTION OF THE WAVE EQUATION WITH FIRST AND SECOND ORDER SOURCE TERMS

From the arguments presented above we may rewrite the simplified wave equation as

$$\nabla^2 p - \frac{p_{tt}}{c_0^2} = -\frac{\beta_0 q_t}{C_{p0}} - \frac{qT_t}{C_{p0}} \left.\frac{\partial \beta}{\partial T}\right|_{T_0} + \frac{\beta_0 p q_t}{\rho_0 c_0^2 C_{p0}} + \frac{\beta_0 q p_t}{\rho_0 c_0^2 C_{p0}} \quad . \tag{2–3.1}$$

Computer programs to evaluate the pressure-time response due to each of these source terms independently and for all of them together were written. To get the total response, the impulse response due to each of the source terms is computed and added. This can be done because the wave equation is linear in pressure and therefore superposition holds.

Figure (2–1) defines the geometry of the laser source-hydrophone system. In this figure, r_0, θ_0, and ϕ_0 are the range and angles defined by the ray connecting the hydrophone to the first column of water insonified by the laser. The source is assumed to be traversing across an air-water interface with a speed of Mach 1.015. Figure (2–2) shows the pressure signal generated at a range of 4 m which is attributable to the leading order source term in Eq. (2–3.1). Figure (2–3) shows the pressure at the same location due to the second term on the right hand side of Eq. (2–3.1). This pressure signal is attributable to the fact that the coefficient of thermal expansion of water varies with temperature (and hence with time for our system). Note that the pressure scale in Fig. (2–3) is 10^{-3} times that in Fig. (2–2). Figure (2–4) shows the pressure signal at the same location which may be attributed to the pressure dependent terms in Eq. (2–3.1). The scale of the pressure axis is the same as that for Fig. (2–3). Note that superposition of these three plots produces a graph which is identical to Fig. (2–2). Hence we conclude that the variation of thermodynamic quantities during the sound

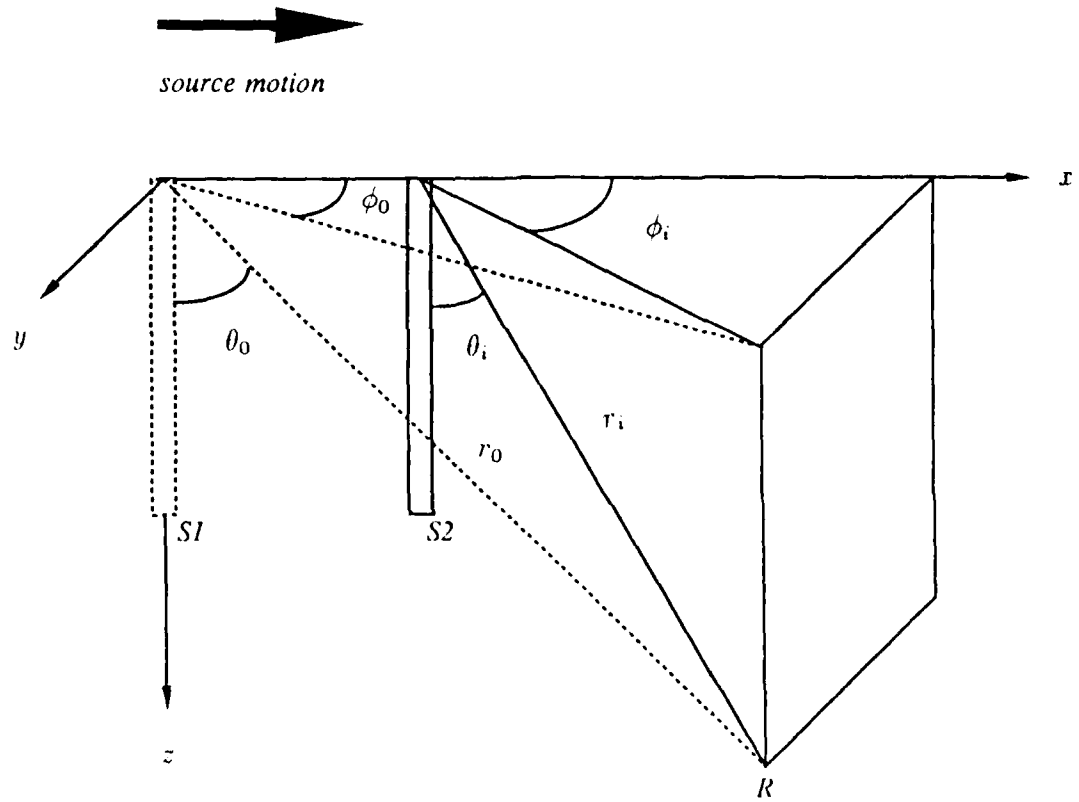

S1, S2 — *source positions*

R — *receiver position*

Figure 2-1 Source-Hydrophone Geometry

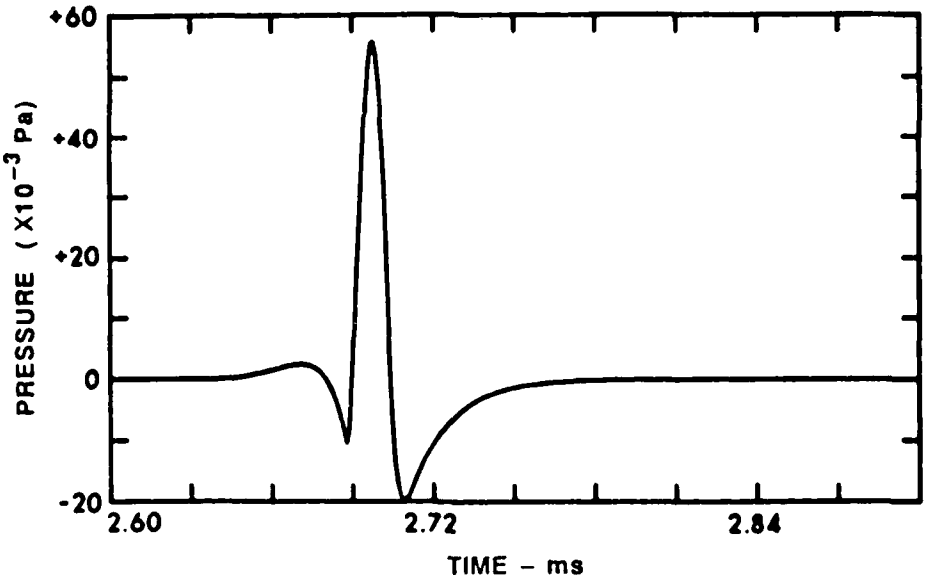

Figure 2 2 Pressure-Time Response due to Leading Order Source Term for a Source Moving at Mach 1 015

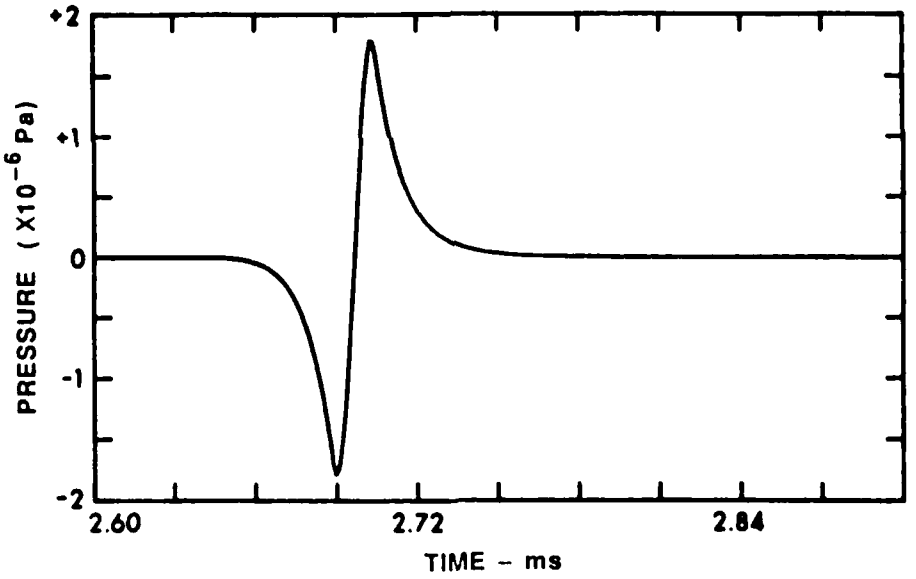

Figure 2 3 Pressure-Time Response due to Time Varying Coefficient of Thermal Expansion for a Source Moving at Mach 1.015

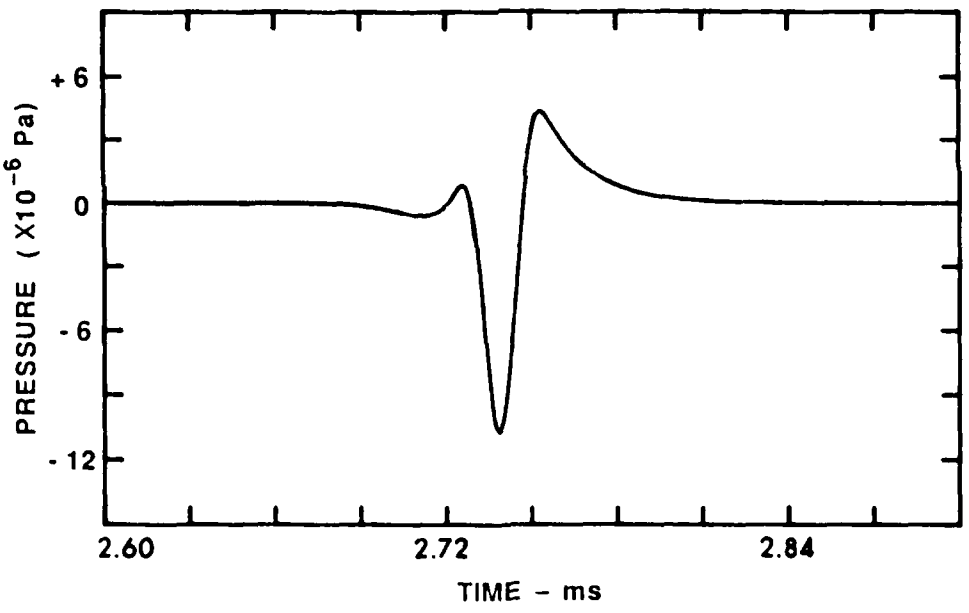

Figure 2 4 Pressure-Time Response due to the Pressure Dependent Terms for a Source Moving at Mach 1 015

generating process is not significant. This dispels all doubts about the significance of the second order terms near Mach 1, since the entire analysis is centered around that source speed.

It should be noted that the analysis contained in this chapter addressed only the effect of nonlinearities in the state equation of the medium. Linear expressions for conservation of mass and momentum were employed. Hence the possibility of convective nonlinearities contributing to the observed unusual behavior of the thermoacoustic source traveling at speeds near Mach 1 has not been eliminated. However it has been reported by Pierce[21] that the effect of hydrodynamic nonlinearities is negligible.

CHAPTER 3

EFFICIENCY CONSIDERATIONS FOR THE THERMOACOUSTIC ENERGY CONVERSION PROCESS

3–1 EFFICIENCY DEFINITION

The question of increasing the transduction efficiencies for thermoacoustic sources has been studied by American and Soviet scientists over the past few years. When the concept of thermoacoustic generation of sound was first conceived, the experimental studies were limited to stationary sources. The main disadvantage of the stationary thermoacoustic source is its low energy conversion efficiency. Figure (3–1), taken from Muir, Culbertson, and Clynch,[5] shows an estimate of the laser power needed to generate given source levels at a distance of 1 m. They predicted that "megawatts of optical power would probably be required in the megahertz frequency region, with gigawatts of power required in the kilohertz region," in order for the transducer to be useful for sonar applications. This low efficiency led to the consideration of a moving thermoacoustic source.

It was reported by Bunkin et al.[6] in 1978 that the amplitude of the acoustic pressure generated in the thermoacoustic process could be increased by moving the laser beam at high velocity through the fluid. A frequency domain approach was used in their analysis which showed significantly increased sound

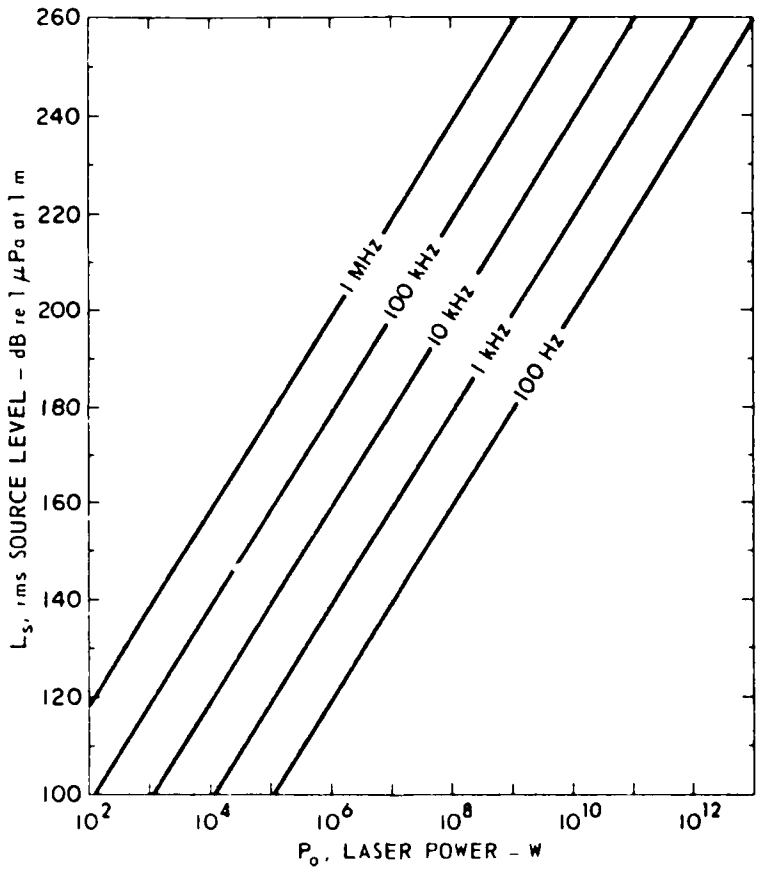

Figure 3-1 Laser Power versus Source Level

pressure levels for a source moving at speeds near Mach 1. Experimental verification of these results was provided. However, in a later article, Bunkin et al.[7] claimed that moving the laser beam does not result in an increased sound pressure level. Again, experimental evidence was offered. Hence, there has been great confusion over the effect of moving a laser source.

In the time domain approach developed by Berthelot and Busch-Vishniac[12] for moving thermoacoustic sources, the acoustic pressure is driven by a source that depends on the time rate of change of laser intensity. Experiments were conducted and the results compared to analytical predictions. It was found that there is good agreement between theory and experiment except for transonic motion of the source, where an experimental enhancement of about 25 dB in the sound pressure level was observed.

Research performed by Pierce and Hsieh[18] on the optoacoustic energy conversion efficiency yielded an energy equation which indicated that the rate of acoustic energy production per unit volume is proportional to the product of the rate of heat addition per unit volume and the local acoustic pressure existing at the same point. This led to the conclusion that the laser energy deposition system should be designed in such a way that a traveling acoustic wave was created, and then its amplitude systematically pumped up by always adding energy at places where the acoustic pressure has a local maximum. We note that the analysis presented in the preceding chapter has shown that if one includes the second order terms associated with entropy generation in the equation of state, then the second order source terms also depend on the product of pressure and another thermodynamic variable. Hence the pumping principle applies to the second order source terms as well as the leading order term.

It was concluded in Chapter 2 that the only term that makes a significant

contribution to the pressure generated by the thermoacoustic source for our laser system is the leading order term. Therefore in the analysis presented in this chapter we ignore all nonlinear effects. With this simplification the energy balance equation can be written as

$$\left(\frac{1}{2}\rho_0 \mathbf{u}^2\right)_t + \frac{p}{\rho_0}\left(\frac{p}{c^2}\right)_t + \nabla\cdot(p\mathbf{u}) = \frac{\beta_0 pq}{\rho_0 C_{p_0}} \quad . \tag{3-1.1}$$

The first and second terms on the left hand side of Eq. (3-1.1) are the kinetic and potential energies per unit time per unit volume of the fluid, respectively. The third term is the work done on the fluid per unit time per unit volume. The term on the right hand side of Eq. (3-1.1) is the heat energy per unit time per unit volume which is converted to acoustic energy. This is in accordance with the law of conservation of energy which states that the input energy either increases the stored energy or is radiated away. Clearly, the higher the fraction of the available laser energy converted to acoustic energy, the more efficient the thermoacoustic process. Hence the efficiency for the process was defined by Pierce[20] as

$$\eta = \frac{\beta_0}{\rho_0 C_{p_0}} \frac{\iint pq\, d\vartheta\, dt}{\iint q\, d\vartheta\, dt} \quad , \tag{3-1.2}$$

where ϑ is the volume of fluid to which heat is added during the thermoacoustic generation of sound.

The interesting property of this efficiency is that the fraction of converted energy depends not only on the heat energy added to the medium, but also on the acoustic pressure of the fluid into which it is dumped. If the laser is intensity modulated, as in the experiments performed by Berthelot,[12] then the heat oscillates in time, producing an instantaneous oscillation of the acoustic pressure. From Eq. (3-1.2) it is clear that this process is not very efficient because the product of pressure and heat oscillates about a low value. Instead, if the laser is

used to always add heat to the fluid which is already at a pressure maximum, then the product of pressure and heat, and therefore the energy conversion efficiency, will be high. If Pierce's argument is valid, one should see a steady increase in efficiency with time under these conditions.

Pierce and Hsieh[18] have examined the use of this pumping principle in light of currently available lasers. They have concluded that even within the limitations of existing laser technology, it should be feasible to develop an airborne laser system that will create detectable sound at ranges up to 10 km or greater.

3–2 NUMERICAL COMPUTATION OF EFFICIENCY FOR THE THERMOACOUSTIC PROCESS

We have numerically evaluated the expression for efficiency given by Eq. (3-1.2) by modifying the program written by Berthelot.[19] The linear first order wave equation for thermoacoustic generation of sound, derived by Larson,[13] is used for calculating the pressure using a convolution approach. The heat input per unit time per unit volume, q, is given by Eq. (2-2.5). The volume integral in Eq. (3-1.2) is evaluated over the laser irradiated region.

If the radius of the laser beam is a, the laser pulse duration τ_p, the speed of the laser across the water surface v, and the optical coefficient of absorption α, then the laser heated volume is approximately a parallelepiped of dimensions $2a$, $v\tau_p$, and $1/\alpha$, as shown in Fig. (3-2). The only irradiated area neglected by this approximation is that corresponding to two half-cylinders extending outward from the edges normal to the y-axis. Using the reference frame indicated in Fig. (3-2), the following inequalities are valid for the laser heated zone:

$$0 < x < v\tau_p \quad , \quad -a < y < a \quad , \quad 0 < z < 1/\alpha \quad .$$

Consider an element $O(x, y, z)$ of the fluid heated by the laser as shown in Fig.(3-3). The polar coordinates for this element are

$$r = \sqrt{x^2 + y^2 + z^2} \quad , \tag{3-2.1}$$

$$\theta = \arccos(z/r) \quad , \tag{3-2.2}$$

$$\phi = \arccos\left(\frac{x}{\sqrt{x^2 + y^2}}\right) \quad . \tag{3-2.3}$$

The point O is heated for a time from

$$t_i = \frac{x - \sqrt{a^2 - y^2}}{v} \quad to \quad t_f = \frac{x + \sqrt{a^2 - y^2}}{v} \quad .$$

Therefore the time integral for the efficiency for point O is evaluated with the limits t_i to t_f since at any time outside that range the added heat (and thus efficiency) are zero. Note that these limits are independent of z.

In order to examine the efficiency defined by Eq. (3-1.2) as the source moves at various speeds, we calculate $p(t)$ for every point O in the laser heated zone. The product pq is then accumulated for all such points as a function of time, where q is assumed to decrease exponentially with depth z and to have a Gaussian shading through the beam cross-section. This permits us to calculate the efficiency as a function of time as the laser moves through the volume. In this manner we may compare the efficiencies for subsonic and transonic motions of the laser beam.

Note that the Mach number of the source, as seen by various points in the laser irradiated region, is not a constant. It varies as $M \sin\theta_i \cos\phi_i$, where M is the absolute Mach number of the source and θ_i and ϕ_i are the angles defining the position of a point in the laser heated volume with respect to the initial source

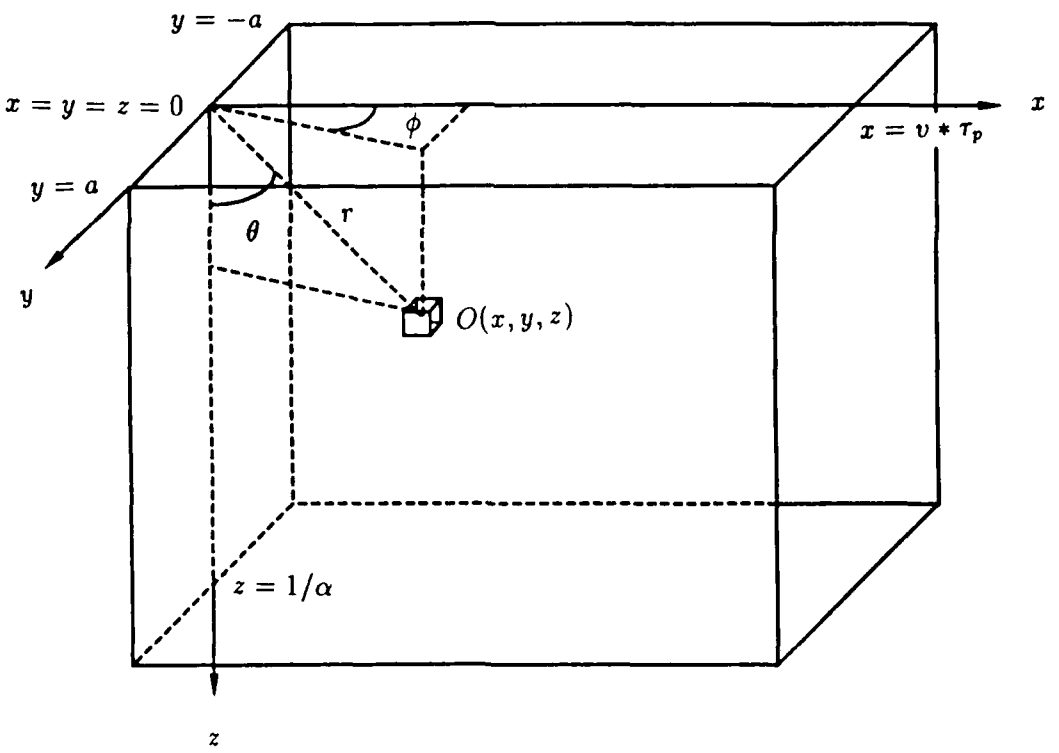

Figure 3-2 Laser Heated Region

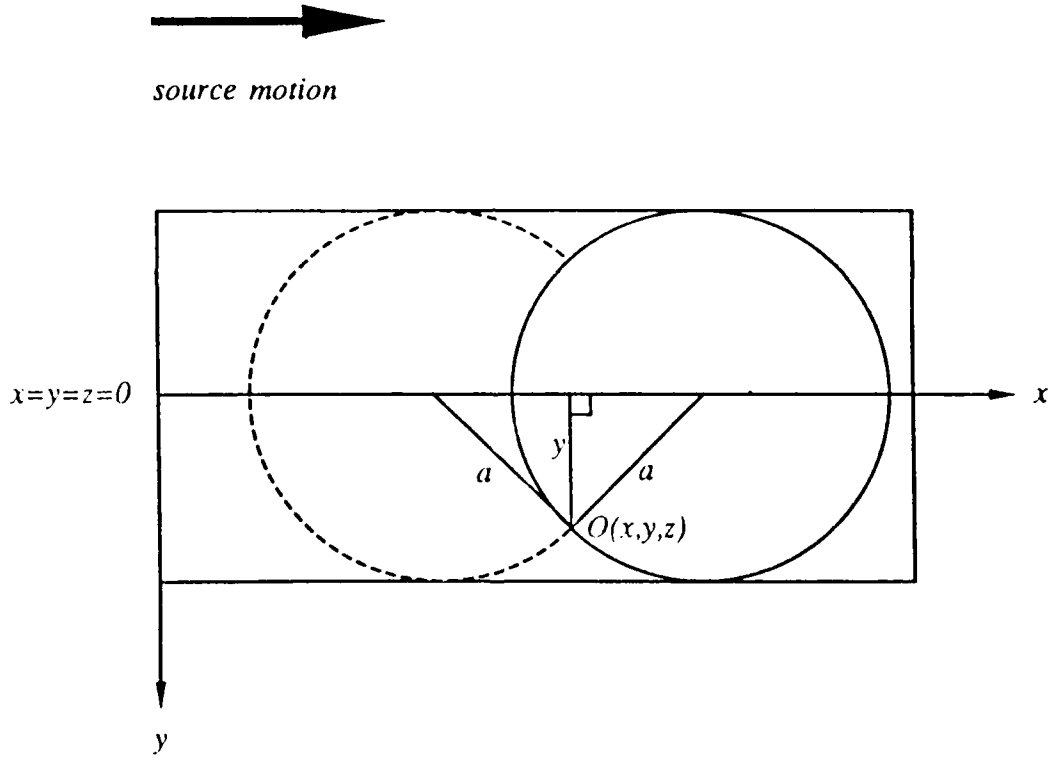

Figure 3 3 Laser Beam Traversal

position. For a constant value of M, it can be shown that $M \sin\theta_i \cos\phi_i$ varies from 0 to M for points in the laser heated region.

The computer program written by Berthelot[14] for calculating the pressure-time response has been modified so as to calculate the efficiency as a function of time. In this calculation, the system properties are all fixed, and the efficiency is found with the time varying from $\tau_p/10$ to τ_p in steps of $\tau_p/10$. The laser is assumed to be unmodulated and identical to that described in Chapter 2. Calculations of the laser-generated pressure are carried out at 1000 points in the laser heated volume. It is to be noted that the actual value of acoustic pressure, including its phase, is used in the calculation of efficiency.

Figure (3–4) shows the variation of normalized efficiency with time for the source moving in a straight line at Mach 0.5. The normalized efficiency is simply the efficiency defined in Eq. (3-1.2) divided by the constant $\mathcal{B}_0/(\rho_0 C_{p0})$. The time axis corresponds to the time after the laser has been turned on at which the efficiency is calculated. The graph shows a rapid decrease in efficiency with time at the beginning of the motion of the laser. This is caused by the fact that the pressure signal has a large negative portion immediately following the positive peak (see Fig.(2-2)). These two peaks thus roughly cancel one another in the integral over time of the product of pq. This large pressure dip is due to the presence of the air-water interface which causes substantial diffraction and diffusion. After the high amplitude portion of the pressure signal is passed, there is a very modest gain in efficiency.

Figure (3-5) is a plot of normalized efficiency versus time for the source moving near Mach 1. This plot indicates a trend similar to that for Mach 0.5. However, it is seen that the maximum value of efficiency for the transonic source is lower than that for the subsonic source.

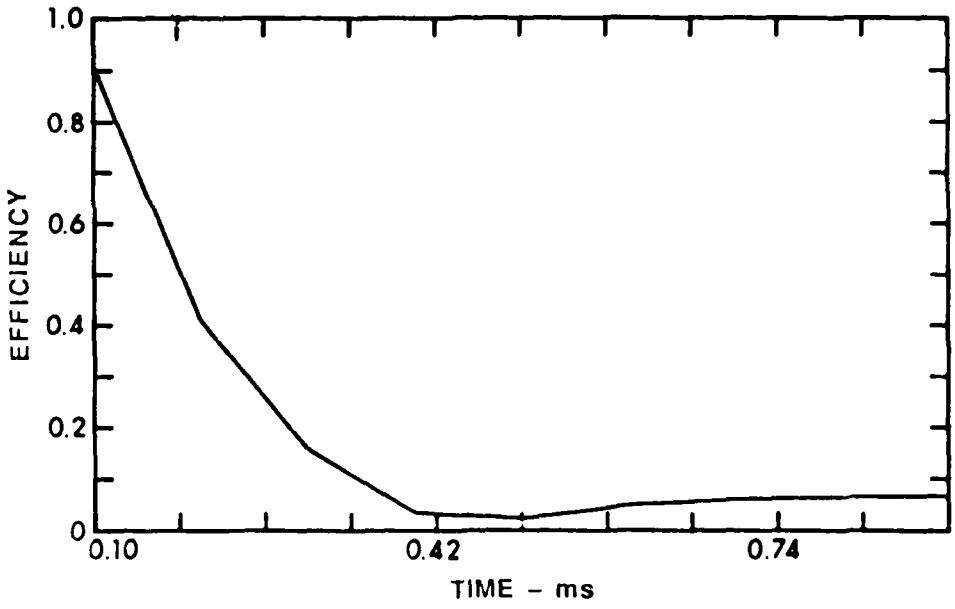

Figure 3-4 Efficiency versus Time for Mach 0.5

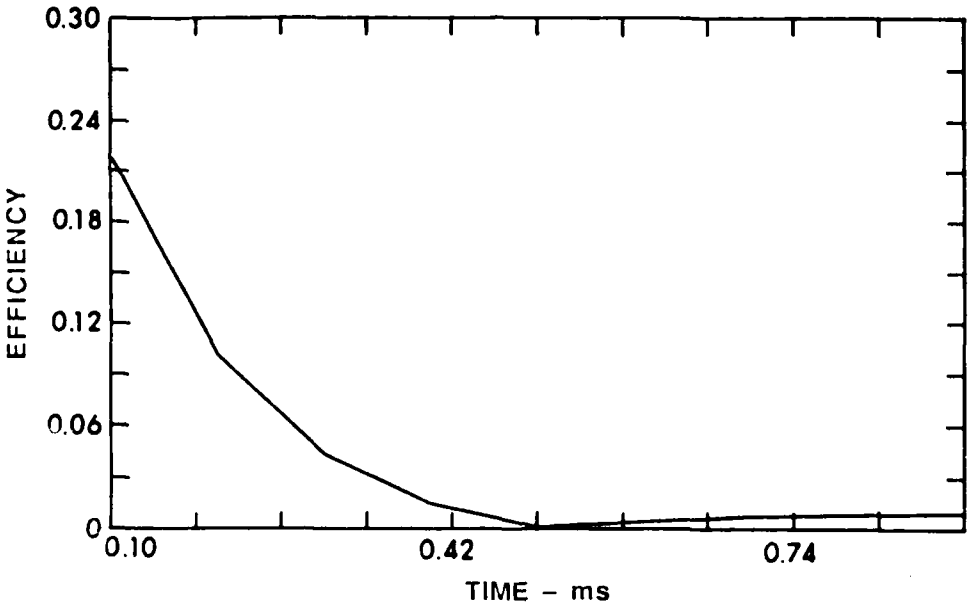

Figure 3 5 Efficiency versus Time for Mach 1.035

The efficiency as defined by Eq. (3-1.2) is zero for a supersonic source because the laser is always heating a region of water which has not yet received sound from previously heated water. Hence, we conclude from Figs. (3-4) and (3-5) that there is no evidence that moving a laser source at Mach 1 increases the sound generating efficiency compared to a subsonic source. In fact, there is evidence to the contrary.

CHAPTER 4

EXPERIMENTAL TESTS

The time domain analysis presented by Berthelot and Busch-Vishniac inherently assumes the superposition principle to be valid in the numerical computation of the acoustic pressure generated by a moving thermoacoustic source. In their approach, the total travel of the laser beam is decomposed in time. Figure (4–1) shows the thermoacoustic source at various points in time as it moves across the water surface in a straight line. The time interval between two successive source positions corresponds to Δt, which can be chosen at will in order to obtain a satisfactory approximation for the continuous source motion. The pressure signal at the receiver is computed by summing the signals generated from each of the source positions during the time the laser is on, taking into account the time delay induced due to the source motion. Thus the total pressure at the receiver is viewed as a convolution-type summation in the time domain between the impulse response of the system and the optoacoustic source strength.

The method described above was shown by Berthelot and Busch-Vishniac to work well for subsonic and supersonic motions of the source. However, for the transonic case, the numerical predictions seem to underestimate the measured sound pressure level by about 25 dB. This discrepancy raised doubts about the validity of the superposition principle for transonic motion of the source. It was

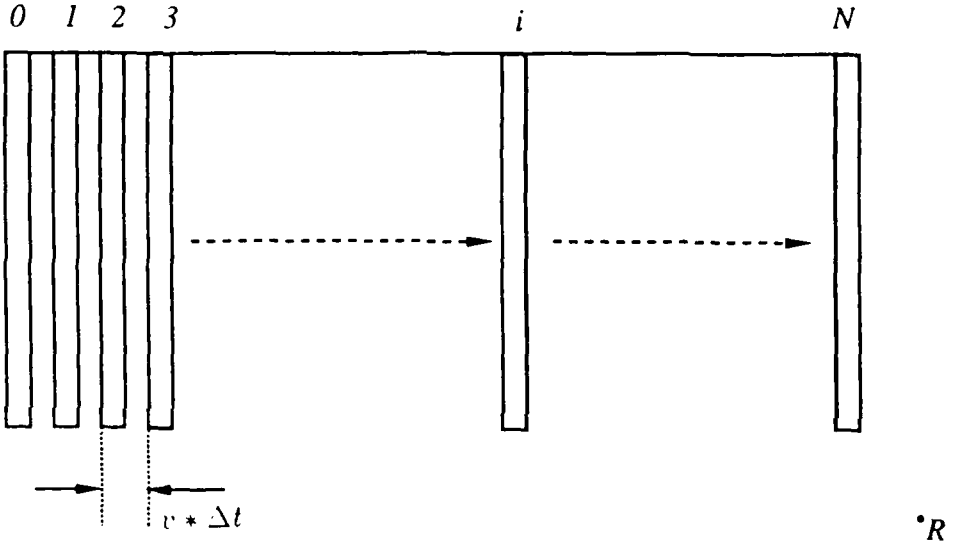

$$p_T(t) = \sum_{i=0}^{N} p_i(t - i\Delta t)\Delta t$$

Figure 4 1 SOURCE POSITIONS DURING SOURCE MOTION

suspected that nonlinear effects dominate near Mach 1, and therefore that the superposition principle might not be valid.

This chapter attempts to clarify the questions raised about application of the superposition principle. Specifically, experimental data are presented for the pressure-time response under two conditions: continuous motion of the thermoacoustic source for a period of roughly 1 ms, and the pressure-time response formed by superposing the signals generated by traversing nonoverlapping portions of the identical path. In the latter case, sufficient time is allowed to elapse between the excitation of the path segments so that interaction is eliminated. Experiments were performed for subsonic, transonic, and supersonic motions of the thermoacoustic source.

4–1 DESCRIPTION OF EXPERIMENT AND EQUIPMENT USED

The apparatus used in our study is the same as that used in earlier studies on moving thermoacoustic sources by scientists at Applied Research Laboratories, The University of Texas at Austin (ARL:UT). The main components include a high power laser source, intensity modulation system, a rotating mirror with a variable frequency power supply, a hydrophone, and an oscilloscope. Figure (4–2), taken from Ref. 22, is a schematic of the experimental setup. A brief description of the various components is given in the following sections. A detailed explanation of the apparatus is given in Culbertson, Chotiros, and Berthelot.[22]

4–1.1 LASER

The laser used in our experiments was procured from Apollo Lasers, Inc. Figure (4–3) shows the optical train configuration for this laser. The laser cavity can accommodate either a Nd:glass rod or a ruby rod. For simplicity, a

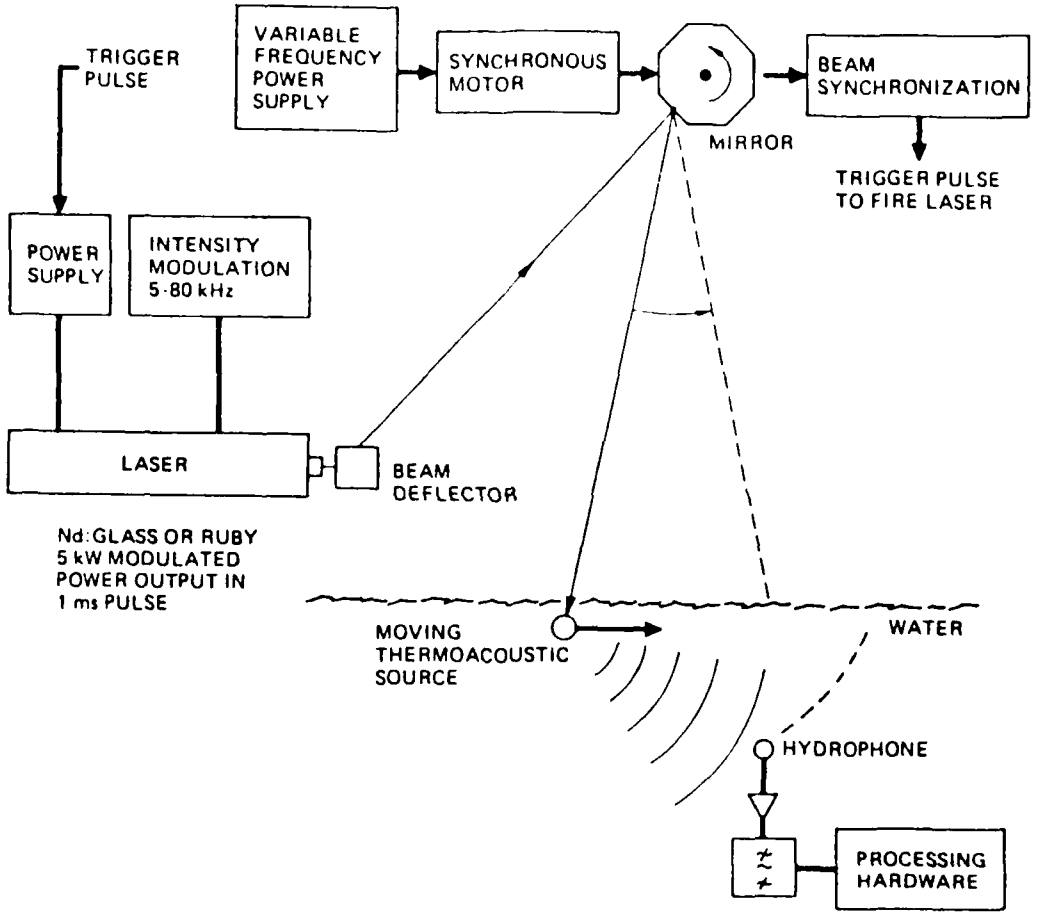

Figure 4.2 Schematic of the Experimental Setup

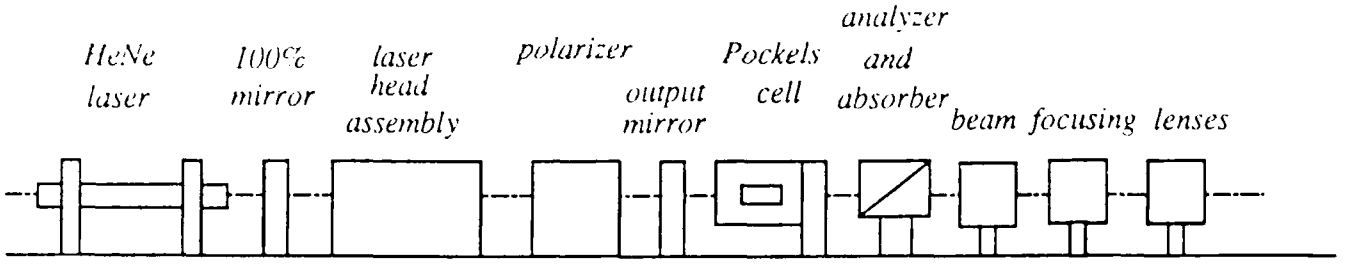

Figure 4-3 Optical Train Configuration

Nd:glass rod was used throughout our experiments. The wavelength of the light emitted by the laser with a glass rod is 1.06 μm. Optical pumping of the glass rod is achieved by a flashlamp. Modulation of the light intensity is affected by polarizing the laser beam by a Brewster stack before it strikes a Pockels cell and a prism analyzer. Figure (4-4), taken from Culbertson, Chotiros, and Berthelot,[22] depicts the principle of laser beam modulation. The Pockels cell consists of an electrically driven KD*P crystal immersed in a protective dielectric fluid. When a voltage is applied to the terminals of the Pockels cell, the plane of polarization of light passing through it is rotated by an amount which is related to the applied voltage. The output of the polarizer, Pockels cell, and analyzer system is given by the relation

$$I = I_0 \sin^2 \frac{\pi V}{2V_{1/2}} \quad , \tag{4-1.1}$$

where I is the transmitted light intensity, I_0 is the incident light intensity, V is the applied voltage, and $V_{1/2}$ is the half-wave voltage of the KD*P crystal (6 kV for the KD*P crystal used). The normalized envelope, $I_0(t)$, of the laser intensity in the experiment is described by the relation

$$I_0(t) = 10.8(t/\tau_p)\ \exp(-5.0t/\tau_p) \quad . \tag{4-1.2}$$

where τ_p is the laser pulse duration. Figure (4-5) illustrates the variation of $I_0(t)$ with time.

As shown by Eq. (4-1.1), there is no light output by the modulation system when $V = 0$. When $V = V_{1/2}$, the laser beam passes through the modulation system with its intensity unchanged. With this configuration, then, the beam can be turned on by a square pulse of amplitude $V_{1/2}$. The duration for which the beam remains in the water is controlled by the width of this square pulse.

The laser beam thus obtained passes through three lenses mounted on

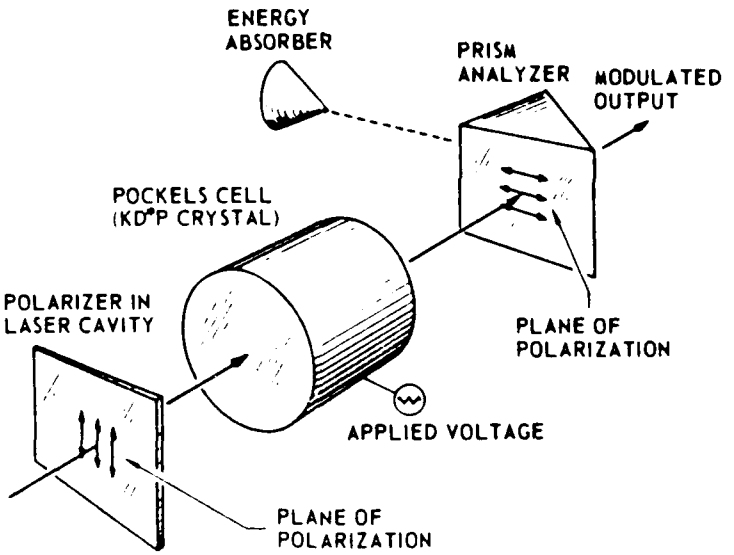

Figure 4-4 Laser Beam Modulation

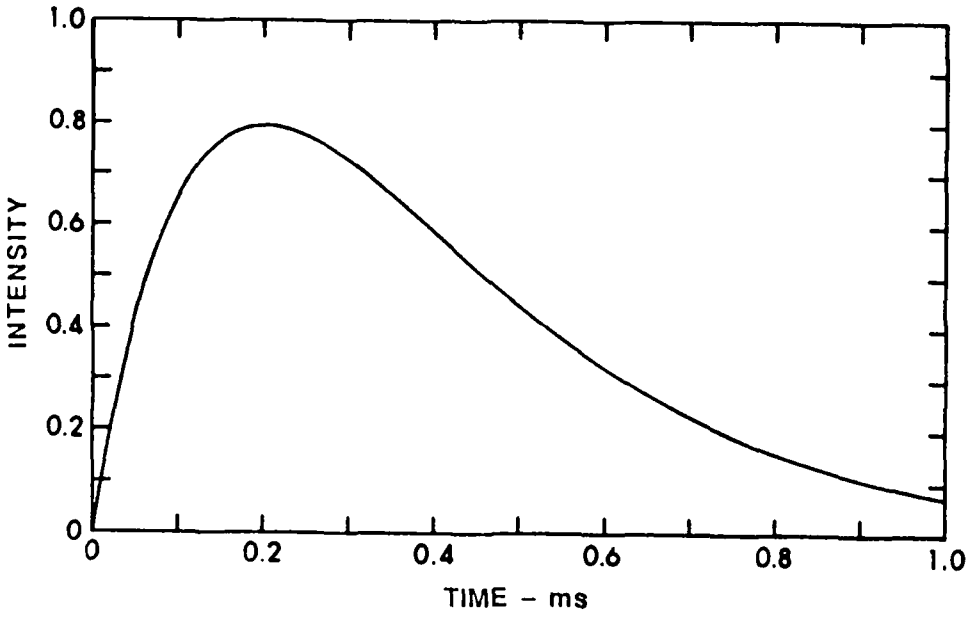

Figure 4 5 Unmodulated Laser Intensity

the covered optical rail. The three lenses, two convex and one concave, aid in bringing the laser beam to a sharp focus on the water surface. The diameter of the beam and its power were optimized to get a sufficiently narrow and powerful beam on the water. A narrow beam minimizes diffraction effects and a powerful beam generates a stronger pressure signal. A computer program was used to calculate the positions of the various lenses relative to the glass rod, in order to obtain acceptable values for the diameter and power of the beam. The beam is finally deflected onto the water surface by a 90° prism and the rotating mirror. A low power HeNe laser is used to align the optical components. The rotational speed of the hexagonal mirror is adjustable to get linear source velocities corresponding to the range Mach 0.1 to Mach 2.6 relative to the sound speed in water.

4–1.2 FIRING CONTROLLER

The firing of the laser is designed to occur at a time such that the beam is initially vertical. The laser beam then moves towards the receiver for the duration of the laser pulse. This coordination is achieved by means of a firing controller designed and built at ARL:UT. Charging of the laser capacitors is controlled manually.

The main function of the firing controller is to generate a pair of pulses: *FIRE* and *OUTPUT*. The *FIRE* signal is a pulse of approximately 100 μs duration and has an amplitude of about 12 V. This signal is used to trigger the laser. The angle at which laser light appears on the water can be selected by a pair of dipswitches. The decimal numbers represented by the two dipswitches are related to the angle, ψ, made by the beam with the vertical at the beginning of the laser sweep, by the following equation:

$$\psi = \pm 120 * (N_{DS1}/N_{DS2}) - 32 + (n * 120) \quad , \qquad (4\text{-}1.3)$$

where the + sign is used when the laser beam is moving away from the laser bench. Similarly, the - sign is used when the beam moves towards the bench. Here, n is a positive integer accounting for the periodicity of the facets on the mirror which is set to zero for simplicity. The angle ϵ can be varied in steps of 120/255 of a degree with 8-bit dipswitches.

The *OUTPUT* signal is a standard *TTL* signal of about 1 ms duration, which is delayed after the *FIRE* pulse. The length of delay can be controlled by another dipswitch. The *OUTPUT* signal is used to trigger the modulating signal produced by the Exact signal generator, which forms the input to the high voltage burst generator. The delay between the *FIRE* and *OUTPUT* signals should be at least 180 μs when a Nd:glass rod is used as the lasing element. This is because there is an intrinsic time interval between the discharge of the capacitor bank and the actual lasing of the rod. The *OUTPUT* signal governs the time at which the laser light appears on the water.

The input to the firing controller comes in the form of a pair of signals from a photodiode assembly placed inside the rotating mirror mounting fixture. The two signals are delayed in time, corresponding to a 60° rotation of the mirror. Continuous rotation of the mirror produces a train of pulses with a period equal to the time taken by the mirror to rotate by 60°. The signal thus obtained is also available as one of the outputs from the firing controller. This is labeled *TPA* and is used to accurately measure and monitor the speed of rotation of the mirror.

4-1.3 RECEIVING AND ANALYZING EQUIPMENT

The pressure signal generated by the moving thermoacoustic source is received by an H-56 hydrophone and viewed on a Nicolet 4094 digital oscilloscope.

The hydrophone is mounted on a vertical fixture attached to a mobile platform in a fresh water tank. The horizontal range and depth of the hydrophone, relative to the initial position of the beam on the water, can be selected at will within the constraints of the tank size. The orientation of the hydrophone is shown in Fig. (4-6). In this figure, xz is the vertical plane and xy is the horizontal plane. $S1$, $S2$, $S3$, $S4$ represent the source positions at the beginning of each interval constituting the total motion of the source. The hydrophone, R, is placed such that the beam moves towards it. Positioning the hydrophone in this manner ensures a reasonably uniform hydrophone response for sound from all points in the laser heated region. The specifications of the hydrophone used in our experiments are:

Model	:	USRD type H-56
Frequency range	:	10 Hz to 65 kHz
Free field voltage sensitivity	:	-171 dB re 1 V/μPa
Preamplifier	:	transistorized, 11 dB gain .

The signal received by the hydrophone is amplified and filtered as needed to get a clean and detectable waveform on the oscilloscope. A Burr-Brown amplifier with a selectable 20-40 dB gain is used for amplifying the raw signal, which is then filtered through a Kronhite bandpass filter.

The voltage-time waveforms thus generated are viewed on the oscilloscope with a sampling rate of 500 ns. The oscilloscope is triggered by a pulse labeled *FIRE SYNC* from the laser control panel. This signal is generated at the instant the laser is fired. The waveforms stored in the oscilloscope's memory are then transferred to minidisks for further analysis on the mainframe computer at ARL:UT.

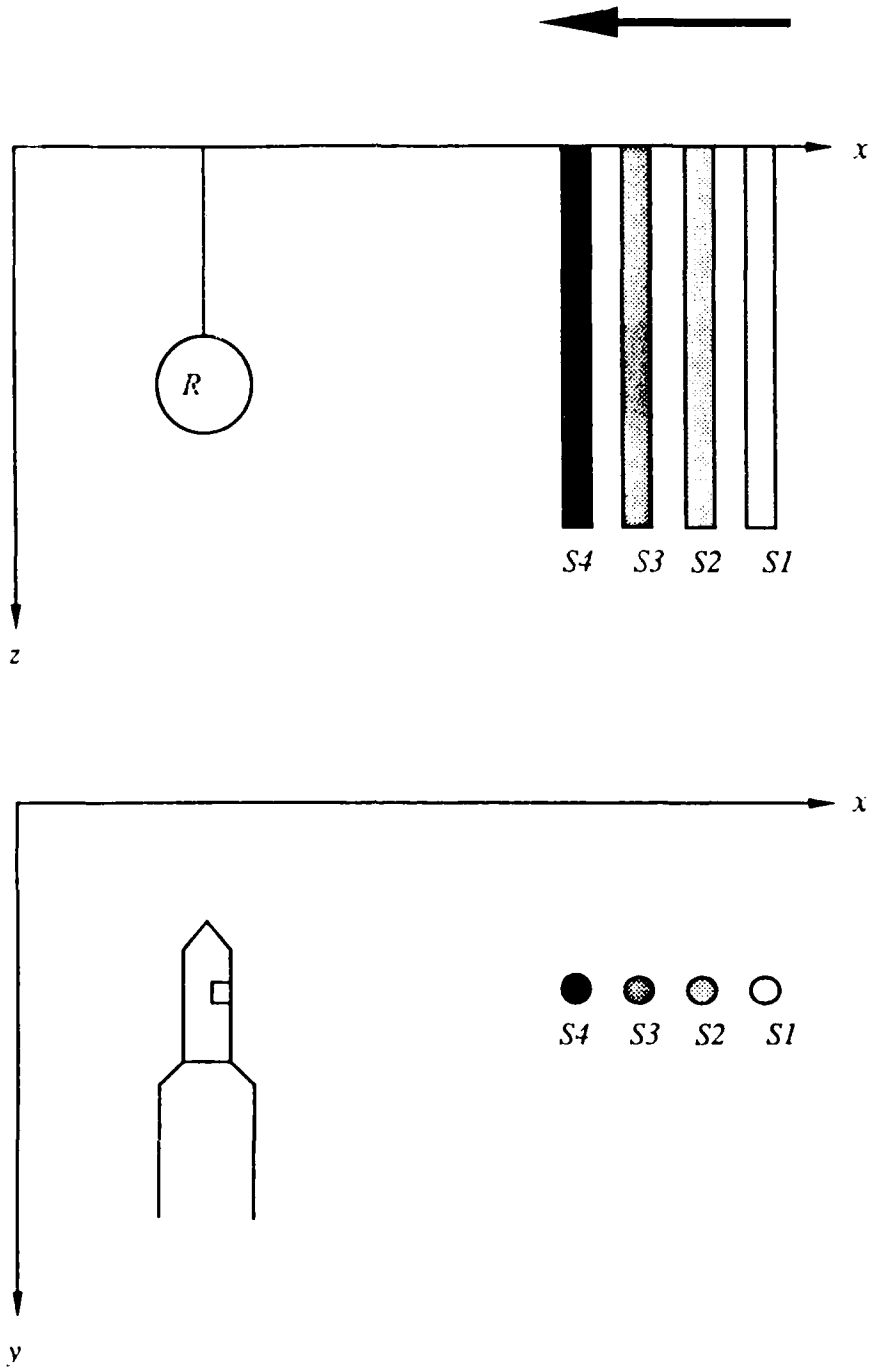

Figure 4-6 Hydrophone Orientation

4–1.4 CONTROL PARAMETERS FOR THE EXPERIMENTS

The laser used in our study had a pulse duration of roughly 1 ms. The maximum energy of the unmodulated laser beam was approximately 20 J. The diameter of the beam on the water surface was of the order of 1 cm.

Experiments were performed for subsonic, transonic, and supersonic motions of the source. The velocities of the source were chosen to correspond to Mach 0.7, 1.0, and 1.3. The hydrophone position relative to that of the source at the beginning of the laser sweep is shown in Fig. (4-7). This position was maintained constant throughout the experiments.

For a typical speed of the source, the laser was first scanned across the water surface for 1 ms. The resulting pressure-time response was recorded. Next, the laser output was tapped from four separate time intervals which, when summed, constituted the laser output for the case of continuous motion for 1 ms. This strategy is indicated in Fig. (4–8), which shows the laser intensity for each time interval. Each interval is roughly 250 μs in duration. The three dipswitches in the firing controller are set to the correct delay between the firing of the laser and the first appearance of laser light on the water; the angle of the beam is set to be vertical when it first strikes the water. A total of four waveforms is obtained for any Mach number of the source. The delay between measurements of these waveforms ensures that the signals they generate are independent. The four waveforms, constituting the complete sweep of the beam, are added together and compared to the waveform obtained by a single laser sweep of 1 ms duration.

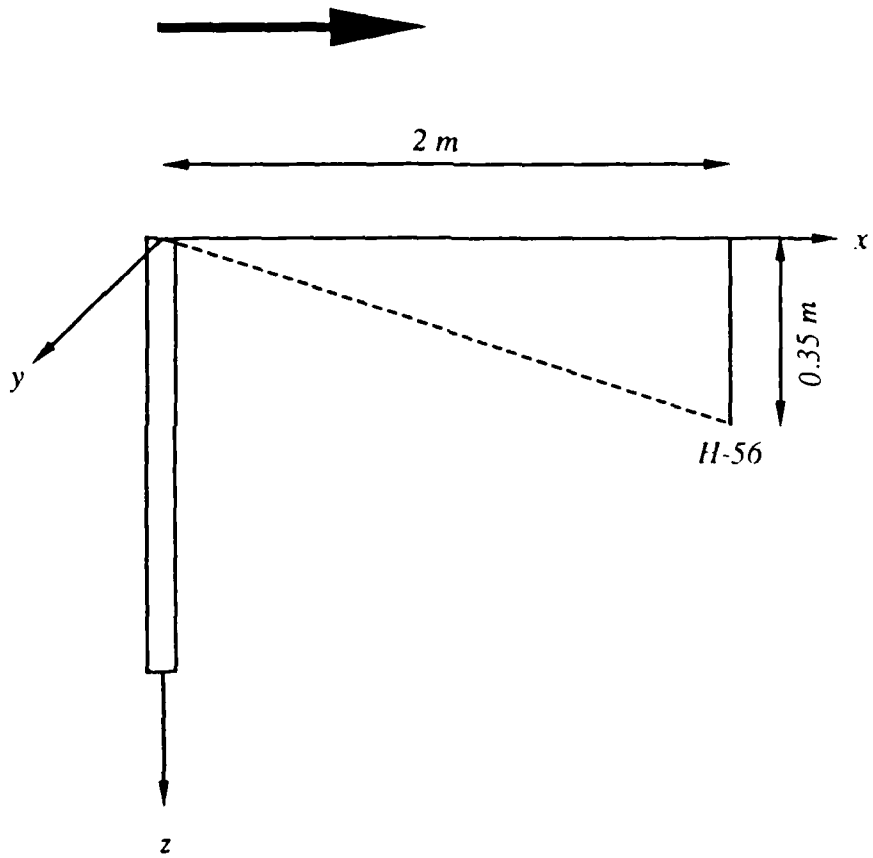

Figure 4-7 Hydrophone Position Relative to the Initially Insonified Water

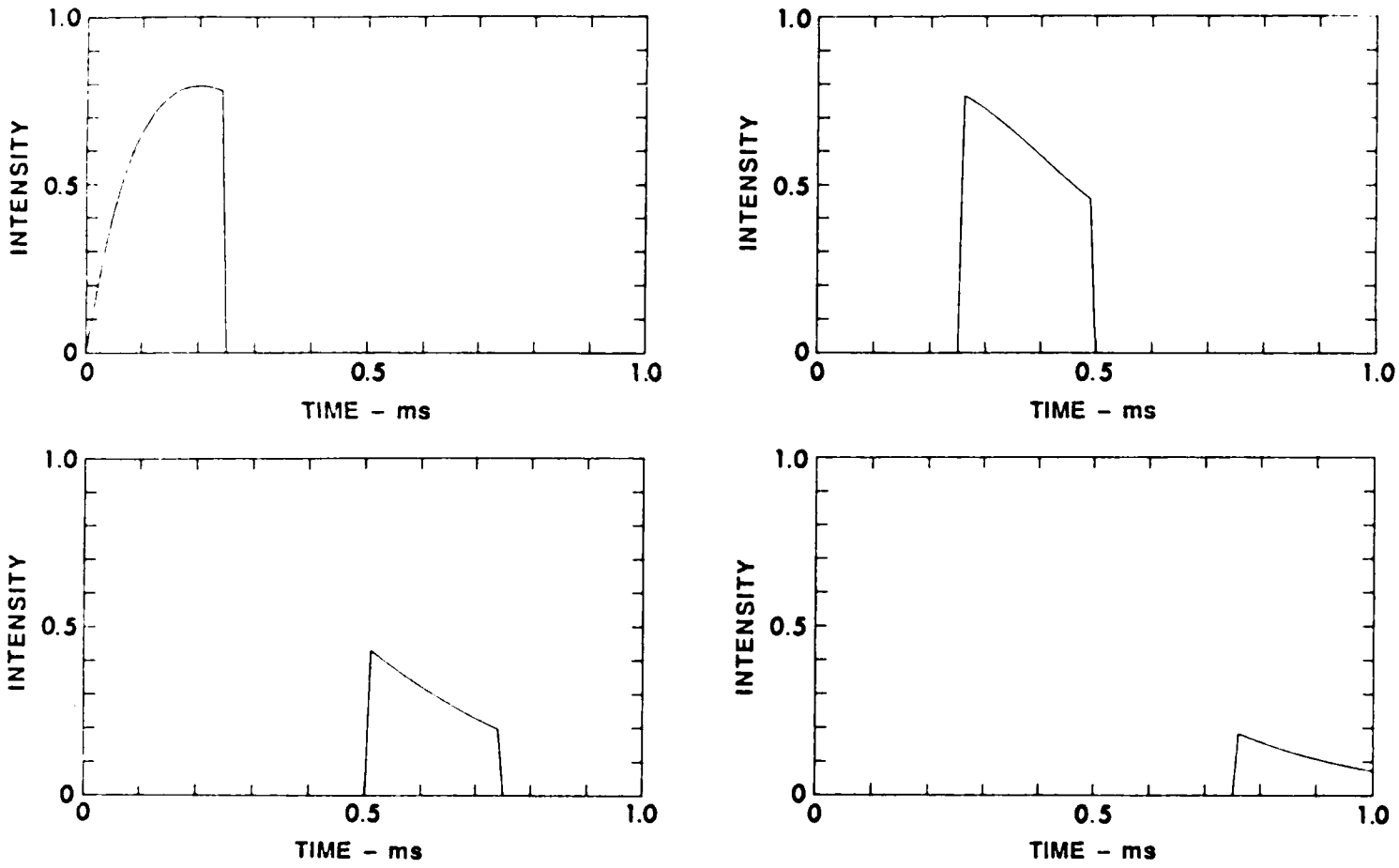

Figure 4 8 Intensity Intervals

4-2 EXPERIMENTAL RESULTS

Figures (4-9) and (4-10) show the sum of the four pieces of the pressure signal and the pressure signal generated by a single sweep of the transonic laser beam, respectively. The signal detected by the hydrophone was captured on disk without any amplification or filtering. Note that there is good agreement between the two pressure signals. The slight variation in amplitude may be attributed to the presence of noise in the vicinity of the hydrophone. This noise accumulates in the sum waveform, thereby increasing its amplitude.

Figure (4-11) shows the composite of the four separate waveforms constituting the entire motion of the source moving at Mach 0.7. Figure (4-12) illustrates the corresponding pressure-time response for the single sweep of the beam for 1 ms. The signals obtained for this case were amplified with a gain of 40 dB and then filtered, the band passed being 11.5 kHz to 100 kHz. Clearly, Fig. (4-11) indicates a higher pressure amplitude compared to Fig. (4-12). This discrepancy might be due in part to the significant contribution to the pressure signal by the amplified noise when the four waveforms are added.

Similar results are noticed for the supersonic motion of the source, but the agreement between the composite shown in Fig. (4-13) and the single sweep pressure signal in Fig. (4-14) for Mach 1.3 is better than that for Mach 0.7. The gain and the filter band for the supersonic case are identical to those for the subsonic case.

A quantitative comparison of the experimental data can be obtained by calculating the rms percent deviation from superposition for various Mach numbers of the source. It is found that the rms deviation is about 267% for Mach 0.7, 255% for Mach 1.3, and 59% for Mach 1.0.

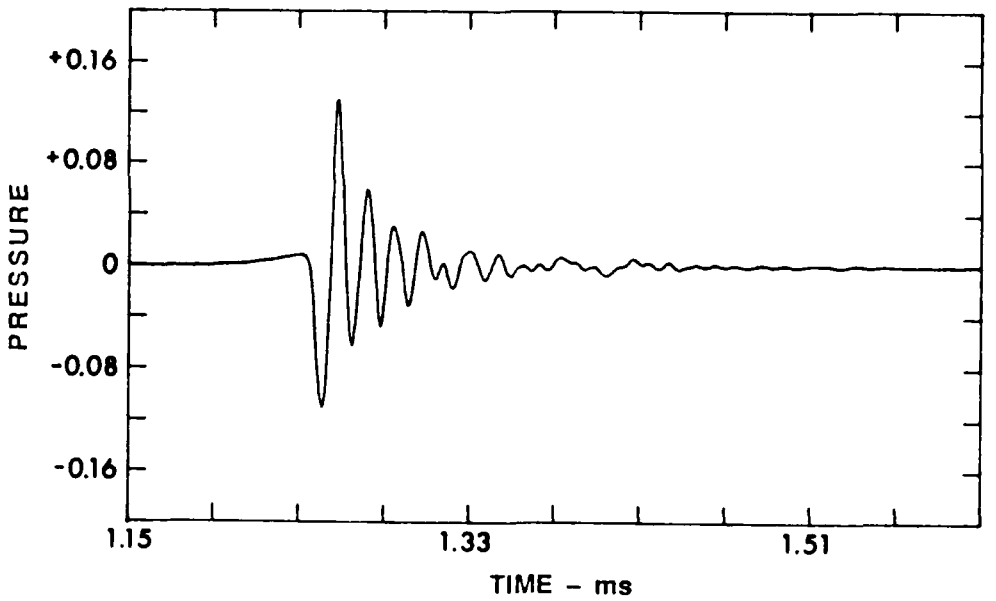

Figure 4 9 Superimposed Signal for Mach 1

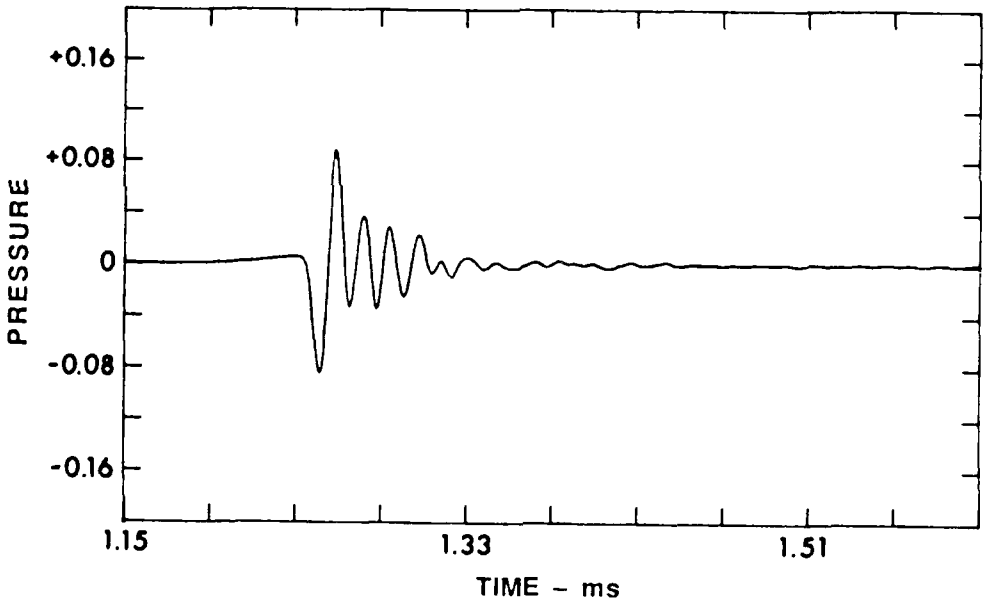

Figure 4-10 Actual Signal for Mach 1

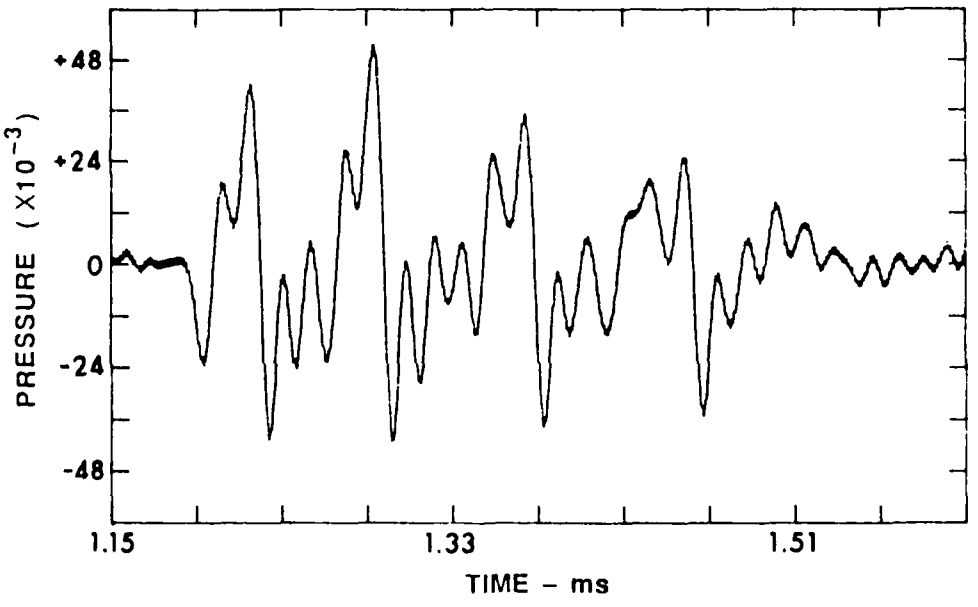

Figure 4 11 Superimposed Signal for Mach 0.7

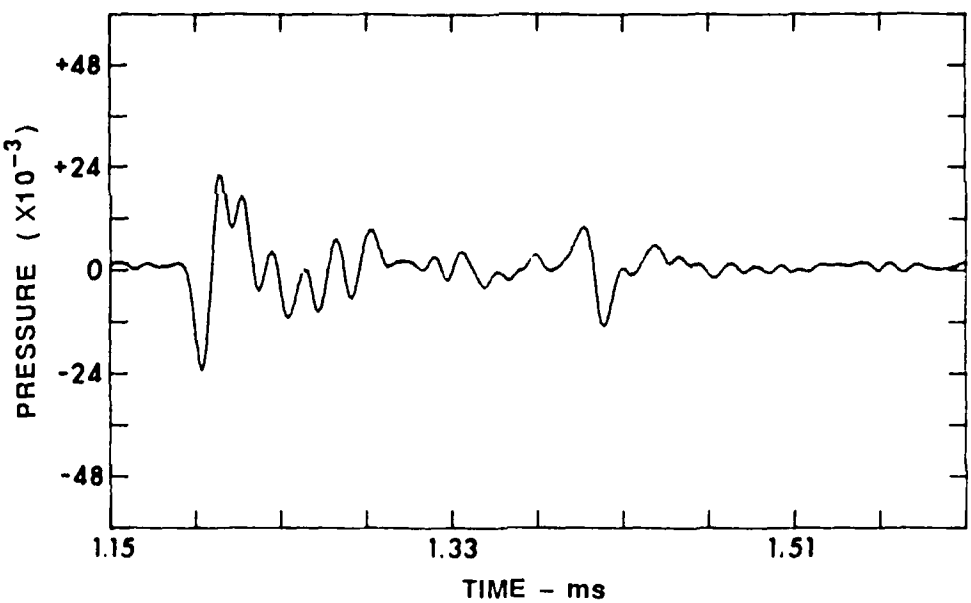

Figure 4 12 Actual Signal for Mach 0.7

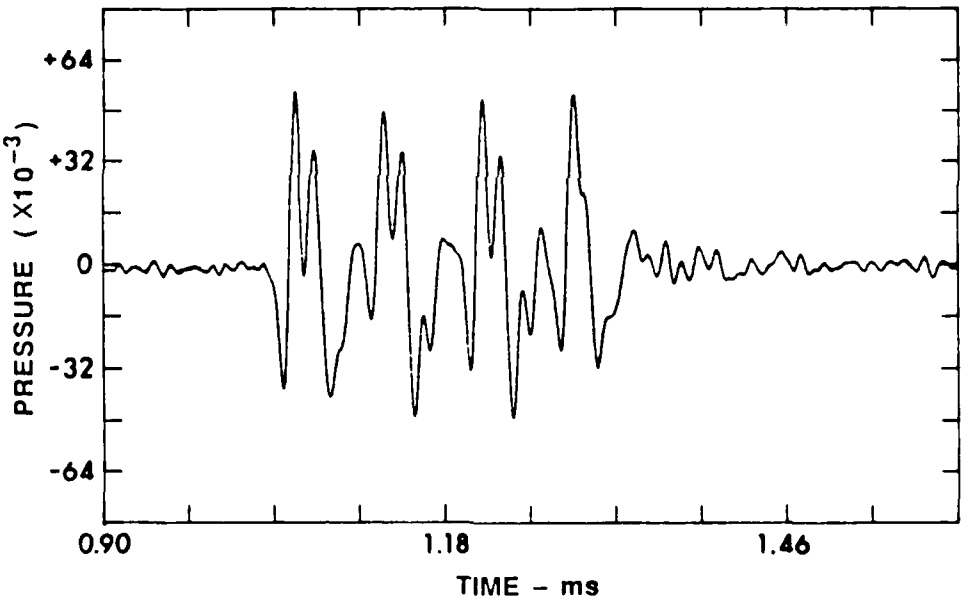

Figure 4-13 SUPERIMPOSED SIGNAL FOR MACH 1.3

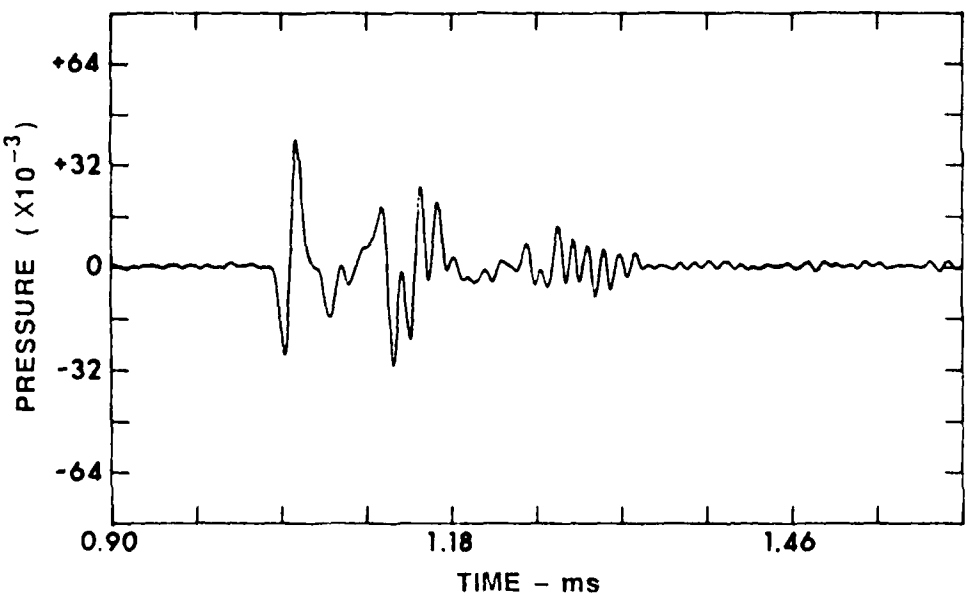

Figure 4-14 Actual Signal for Mach 1.3

The experimental data presented generally support the validity of the superposition principle for subsonic, transonic, and supersonic motions of the thermoacoustic source on the water surface. In particular, we see very good agreement between the composite signal and the continuous signal when the source is moving at Mach 1, as indicated by the rms percent deviation. From this we conclude that there is no evidence to support the supposition that nonlinear effects are the cause of the amplitude magnification observed for a thermoacoustic source traveling at Mach 1.

CHAPTER 5

SUMMARY AND CONCLUSIONS

The main objective of this part of the study was to investigate the prevailing theories concerning the causes of increased sound generation for a transonically moving thermoacoustic source. The approach employed three techniques. First a wave equation was derived in which the leading nonlinearities were retained in the equation of state. Second the efficiency defined by Pierce and Hsieh was numerically determined. Third an experimental check of the validity of the superposition principle was conducted.

The wave equation for sound generation by the thermal mechanism was rederived including the most important second order term in the equation of state. The effects of time varying the thermodynamic properties of the medium were thus considered. The new forcing terms in the wave equation include the effects of a time varying specific heat, coefficient of thermal expansion, acoustic pressure, and temperature. The wave equation was solved numerically with the linear source term and the second order terms involving the coefficient of thermal expansion and the acoustic pressure. The ensuing analysis of the sound field generated by the source does not indicate a significant variation over that obtained by earlier studies on transonic thermoacoustic sources. Therefore it can be concluded that the variation with time of the pertinent thermodynamic quantities,

C_p and β, has little effect on the pressure generated by a moving thermoacoustic source. The linear wave equation derived earlier by Larson[13] with a single first order driving term is perfectly valid for studies on thermoacoustic sources over the entire range of source velocities.

The concept of efficiency for moving thermoacoustic sources has been examined. The efficiency of the thermoacoustic process was defined by Pierce as the fraction of the heat energy that is converted to acoustic energy. It was suggested that moving the source at Mach 1 would significantly improve the transduction efficiency of the thermoacoustic process because of the resulting dumping of heat in regions of pressure maxima. As a direct consequence of this principle, we should expect a monotonically increasing value of efficiency with time during the interval of heat addition. The integrals constituting the definition of efficiency were evaluated numerically and the resulting value of efficiency plotted as a function of time. These plots indicate a rapidly decreasing efficiency with time at the beginning of the signal, for any Mach number of the source. This is because the effect of the air-water interface is to diffuse and diffract the sound wave, thus tending to decrease the efficiency of the process. For later portions of the signal there is a modest increase in efficiency. The plots also show that the efficiency is higher for subsonic motion of the source than for transonic motion.

The experimental studies performed in this research support the assumption that the superposition principle applies for moving thermoacoustic sources. The superposition principle has been verified for subsonic, transonic, and supersonic motions of the source. This supports the theory that the linear wave equation is applicable to this process. Thus we see no evidence to support the prediction that nonlinear effects are important for the transonically moving source.

Reviewing the arguments presented in this part of the report, it is clear

that none of the theories considered was able to explain the observed enhancement of the pressure signal when the source moved at Mach 1. This is because all of them concentrate on the significance of nonlinear effects. The conclusions reached in this analysis indicate the validity of the linear theory.

The results of this investigation, in conjunction with the articles published in Soviet journals, suggest that a more accurate model of the laser intensity distribution across the beam cross-section could provide clues to the unpredictable behavior near Mach 1. Presently, it is assumed that the intensity has a Gaussian shading through the beam cross-section.

Part II

PARAMETRIC STUDY OF A LASER-GENERATED ACOUSTIC SIGNAL

CHAPTER 6

INTRODUCTION

The work on thermoacoustic sources which has been reported in the literature in the last decade has typically concentrated on the efficiency and directivity of the sound generated in this process. Although important, these measures obscure the fact that the sound signal generated by a moving source varies in form as the source-receiver geometry changes. In the research reported here, we study the acoustic signal generated by the moving laser in detail. Properties of the signal are identified and the manner in which these properties change with respect to source and receiver parameters is quantified. This information identifies those aspects of the sound signal that are most and least susceptible to change. If the thermoacoustic source is used for underwater communication in the future, the statistics compiled here should be quite useful.

In the work described here a FORTRAN computer program called MTS, written by Yves H. Berthelot,[19] is used to numerically predict the received acoustic signal. This computer program is based on the time domain approach discussed previously. Various properties of the received acoustic signal, such as maximum and minimum periods and the duration of the received signal, are examined as a function of the source parameters, such as velocity and source-receiver range and angle. This enables us to quantitatively determine which signal properties

are most and least sensitive to source geometry variations. Included in the next section are definitions of the properties of the received acoustic signal which are examined and the parameters which are varied. Results of the numerical study are presented in the following chapter, and conclusions drawn in Chapter 8.

CHAPTER 7

SYSTEM PARAMETERS

The laser assumed to be generating the sound in this part of the study is a Neodymium:glass laser identical to the laser discussed earlier. This laser has a wavelength of 1.06 μm, and a corresponding optical coefficient of absorption, α, of 13.7 Np/m in fresh water where the speed of sound, c, is 1486 m/s. The laser pulse duration was set to 0.8 ms, while the laser beam radius was set to 0.5 cm. A Gaussian intensity distribution across the laser beam was assumed.

The parameters of the source which are varied may be classed into two categories: those associated with the source, and those associated with the source-receiver geometry. The parameters of the source which are varied are as follows: (1) the modulation frequency, f, of the laser intensity, shown in Fig. 7-1, and (2) the velocity, v, or Mach number, $M = v/c$, of the laser beam on the surface of the water, as shown in Fig. 7-2.

The parameters associated with the source-receiver geometry which are varied are as follows: (1) the initial distance between the source and the receiver, r_0, (2) the initial horizontal angle, ϕ_i, and (3) the depth of the receiver, h. All of these parameters are shown in Fig. 7-2.

Table 7-1 shows the values of the parameters which were used in the study. All possible combinations of the parameters were used, resulting in a total

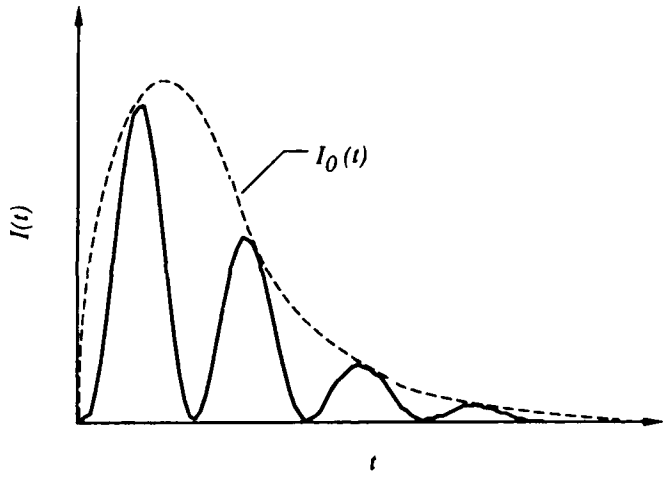

Figure 7 1 Modulated Laser Intensity

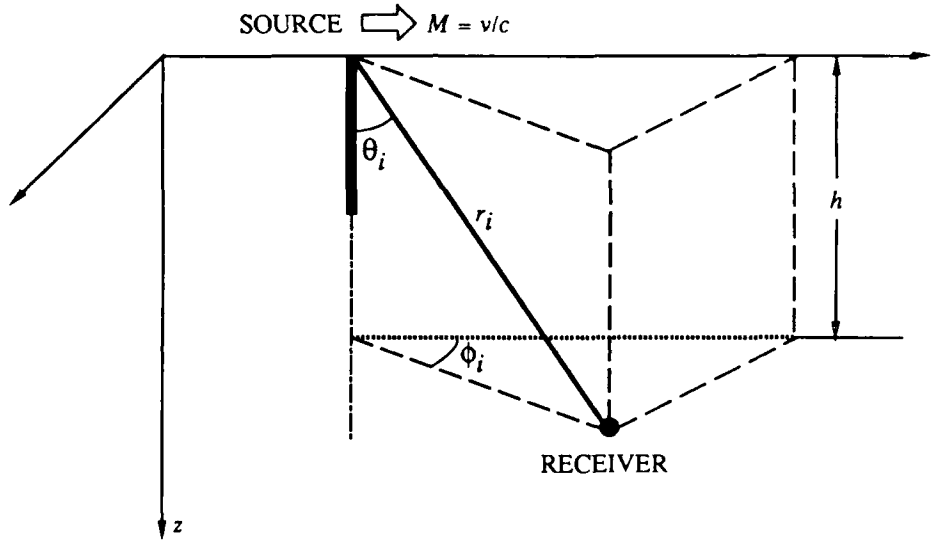

Figure 7-2 Source-Receiver Geometry

r_i (m)	100, 750, 2000
h (m)	5, 15, 40
ϕ_i (deg)	0, 45, 90, 135, 180
M	0, 0.5, 1.0, 1.5, 2.0
f (kHz)	5, 30, 60

Table 7 1 PARAMETER VALUES

of 675 cases. These values of the parameters were carefully chosen to cover the whole range of physically realizable situations. The only limitation on them is that the hydrophone depth, h, is limited to a maximum value of approximately 54 m, since it appears in the argument of the hyperbolic sine function $\sinh(\alpha * h)$ in the program MTS, and the argument itself is limited to a maximum value of approximately 742 on our computer. However, this limitation is a minor one, since depths greater than 54 m are unlikely to be used for hydrophones.

7–1 EXAMINED PROPERTIES OF THE RECEIVED SIGNAL

The examined properties of the received acoustic signal may be placed into two categories: time related properties and pressure related properties.

The time related properties of the acoustic signal which were numerically investigated are as follows:(1) the duration of the received signal, TD, (2) the time at which the absolute peak pressure occurs, TPK, with zero time defined as the time at which the received signal begins, (3) the maximum period in the signal, $TMAX$, found from zero crossings of the signal, (4) the minimum period, $TMIN$, (5) the average of all periods, $TAVE$, and (6) the ratio of the time at which the peak pressure occurs to the duration time, TPK/TD. As will be discussed, TPK/TD is a measure of the amount of time inversion of the signal.

These properties are shown in Figs. 7-3(a) and (b). The beginning and end of the received signal are defined as the points where the sound pressure level of the signal, L_p, has dropped to 40 dB below the L_p of the absolute peak pressure. Because of noise inherent in a real signal, computing the first and last periods would be difficult. Therefore they were not considered in this study unless the signal contained only three periods. In this study that only occurs when the

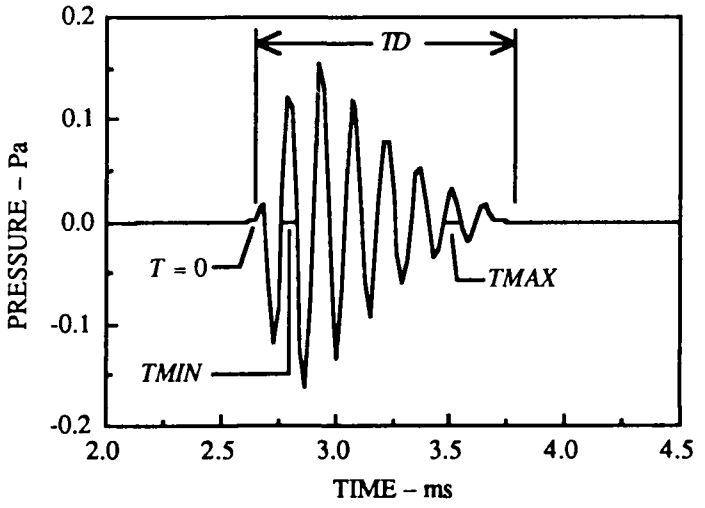

(a)

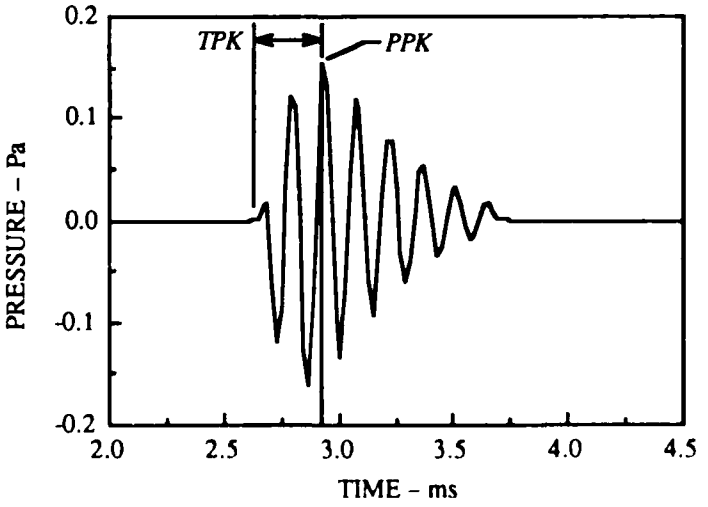

(b)

Figure 7 3 Pressure and Time Properties

ARL UT
AS-87-323
LJG - GA
4 - 9 - 87

Mach number as seen by the receiver, RM, is approximately equal to one. The Mach number observed by the hydrophone is defined by $RM = M \sin\theta_0 \cos\phi_0$ where $\theta_0 = \arccos(h/r_t)$ (Fig. 7-2 shows how θ_0 and ϕ_0 are defined). Note that RM only equals the Mach number of the laser beam when the source is moved in a straight line directly toward the hydrophone.

The pressure related properties which we examined are as follows: (1) the absolute peak pressure, PPK, as shown in Fig. 7-3(b), (2) the root mean square pressure, $PRMS$, of the acoustic signal, and (3) the pressure ratio, $PPK/PRMS$.

In order to obtain the pressure and time properties just described, approximately 110 FORTRAN lines were added to the already existing MTS program. This code solves for the pressure signal as a function of time using the previously described convolution-like approach. In general, with a time step of 0.671 μs, each case took approximately 16 minutes to run on a CYBER 830 Control Data Corporation computer system located at ARL:UT.

CHAPTER 8

RESULTS OF NUMERICAL STUDY

In this chapter we present the numerically obtained results for the variation of the signal properties as the source and geometric properties of the laser sound system are varied. Each signal parameter is discussed independently in terms of its sensitivity to changes in the system characteristics.

8–1 TIME RELATED PROPERTIES

8–1.1 DURATION TIME, TD

The numerical results obtained for TD are shown in Fig. 8–1. Figure 8–1 is typical of the figures that will be presented in this chapter. A total of seven graphs are presented, each displaying TD versus ϕ_0. In each graph there are five curves, each corresponding to a different source velocity.

Figures 8–1(a)–(g) show that TD is quite sensitive to changes in the initial horizontal angle, ϕ_0, and the Mach number, M, of the laser beam on the surface of the water. Both of these variables affect the apparent Mach number of the source as observed by the hydrophone, so the sensitivity of TD to them comes as no surprise. However, note that TD is not sensitive to changes in the angle ϕ_0 when $M = 0$ since the stationary source radiates sound omnidirectionally. TD

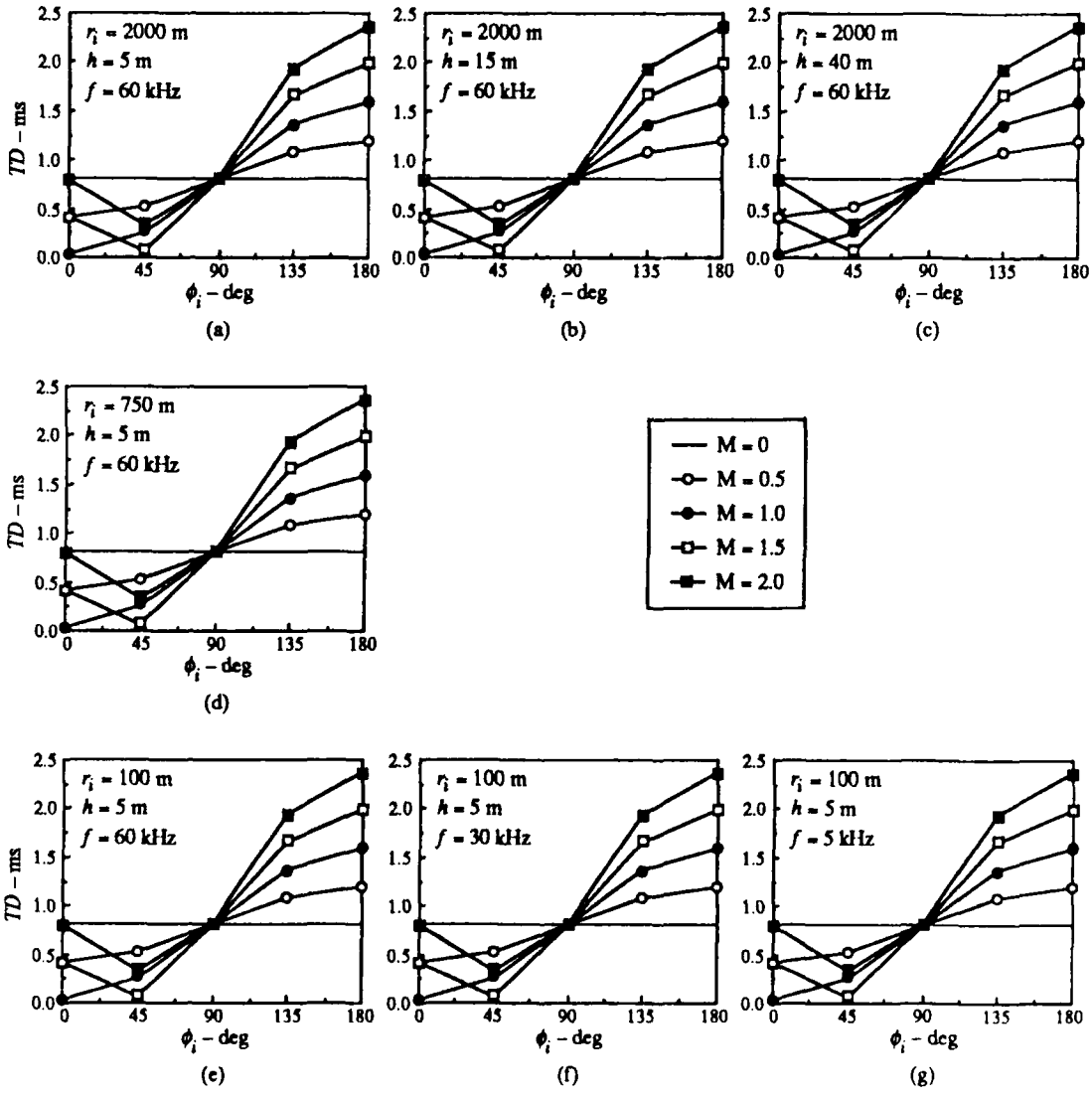

Figure 8-1 Duration of Received Signal

generally becomes more sensitive to changes in ϕ_0 as M increases from 0 to 2 since the source tends to become more directive as the source speed increases.

We also note that TD is least sensitive to changes in M when $\phi_0 = 90°$ so that the laser beam moves in a path normal to the line connecting the hydrophone and the starting point of the laser. The apparent Mach number, RM, under these conditions, begins at zero and slowly increases as ϕ_i changes. From the data for the cases with $\phi_0 = 90°$ we see that TD increases slightly as M increases from 0 to 2, since the range of angles of ϕ_i increases, but the difference between TD for $M = 0$ and $M = 2$ is only on the order of 2%. Note that TD generally becomes more sensitive to changes in M as ϕ_0 decreases from 90° to 0°, and increases from 90° to 180°. Restated, TD is most sensitive to changes in M when the laser is moving directly towards the receiver, or directly away from the receiver.

Viewing Fig. 8–1, we conclude that the d ration of the signal increases monotonically as the laser moves away from the receiver, that is, when ϕ_i is in the range of 90–180°, and that the maximum duration of the received signal occurs when $M = 2$ and $\phi_0 = 180°$. This result can be explained by the fact that if the source is moving away from the hydrophone, then the distance which the last wavelet must travel from source to receiver increases as the velocity of the source increases, and is greatest when the laser is moving directly away from the receiver.

Finally, an explanation can be given of the manner in which TD varies as the laser moves towards the receiver, that is, when ϕ_0 is in the range of 0 – 90°. In this region, the received signal becomes more compressed in time as RM increases from 0 to 1, and will then become less compressed as RM increases further. The shortest duration of the signal should then occur near $RM = 1$, since for this case the whole signal arrives at the receiver essentially at the same time. The duration of the signal increases as RM becomes greater than one, because

the distance which the last wavelet must travel to reach the receiver decreases as the velocity of the source increases. Therefore, the last wavelet emitted by the source arrives at the receiver increasingly earlier than the first wavelet emitted by the source as the velocity of the source increases. The result is that the signal duration increases with the source velocity. Proof of this is shown in Fig. 8-2, which displays TD versus RM for one set of system parameters.

Figures 8-1(a)-(c) represent identical cases except for the depth of the receiver. From these three graphs one sees that TD is very insensitive to changes in the depth, h, of the receiver. The data for these cases reveal that TD increases slightly as h increases. The increase between the cases for which $h = 5$ m and $h = 40$ m is generally on the order of 0.3%.

The cases used to generate Figs. 8-1(e)-(g) are identical except for the modulation frequency of the laser, f. From these figures we conclude that TD is very insensitive to changes in the modulation frequency. The data for these cases show that the duration of the received signal increases slightly as the modulation frequency increases. The increase between the cases for which $f = 5$ kHz and $f = 60$ kHz was on the order of 0.6%. This slight increase in TD as f increases can be explained as follows: Berthelot and Busch-Vishniac[12] have shown that the pressure amplitude of the received signal increases as f increases (as will also be shown later by the pressure related properties). Therefore the beginning and end of the received signal are detected earlier and later, respectively, by the receiver, causing an increase in TD.

Figures 8-1(a), (d), and (e) were generated from identical situations except for the source to receiver initial range. They show that TD is also very insensitive to changes in the initial distance between the source and receiver, r_{si}. The results for these cases show that the duration of the received signal decreases

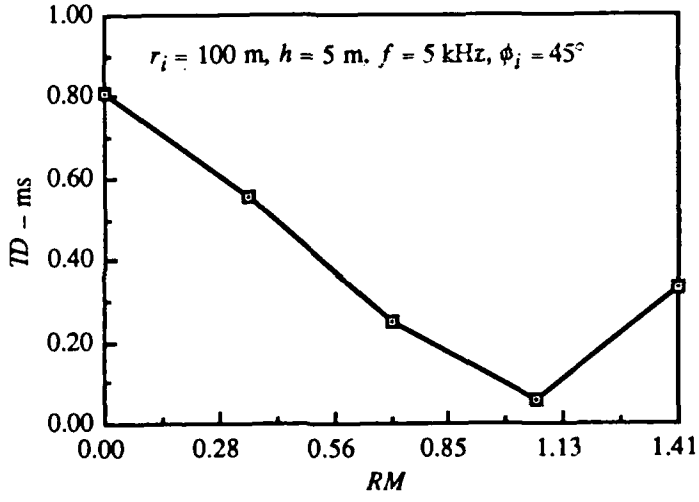

Figure 8 2 Pulse Duration versus Mach Number

slightly as r_0 increases. The difference between the cases for which $r_0 = 100$ m and $r_0 = 2000$ m is generally on the order of 3%. This result can be explained by the fact that spherical spreading will decrease the pressure amplitude of the received signal, and that spherical spreading increases as r_0 increases. Therefore the beginning and end of the received signal are detected later and earlier, respectively, by the receiver, and thus the decrease in TD.

From these results we conclude that the duration of the sound signal generated by the thermoacoustic source is insensitive to changes in r_0, f, and h, but is dependent on the apparent speed of the source as seen by the receiver. In terms of geometrical parameters, this means that the duration of the signal is highly dependent on ϕ_0 and M.

8–1.2 TIME OF PEAK PRESSURE, TPK

Figure 8–3 shows the results for TPK, the time at which the peak pressure is observed. Like the time property TD, TPK is quite sensitive to changes in ϕ_0 and M, as shown by Figs. 8–3(a)–(g). For a stationary source the graphs in Fig. 8–3 show that TPK, like TD, is not a function of ϕ_0 since the same signal would be observed at all angles. However, unlike TD, TPK does not increase monotonically as the laser moves away from the receiver, although there is a pattern in the way TPK varies with M when $\phi_0 = 0°$. Figure 8–4, which displays TPK versus M for a specific case, more clearly reveals this pattern. It is important to note that for this specific case $RM = M \sin\theta_0 \cos\phi_0$ is approximately equal to M, since $\phi_0 = 0°$ and $\theta_0 \approx 90°$. Figure 8–4 shows that TPK decreases as M goes from 0 to 1, and increases as M goes from 1 to 2. This is a result of the signal being compressed in time (Doppler shifted) when $M = 1$ is approached from below and above. This effect of time straining would lead one to expect

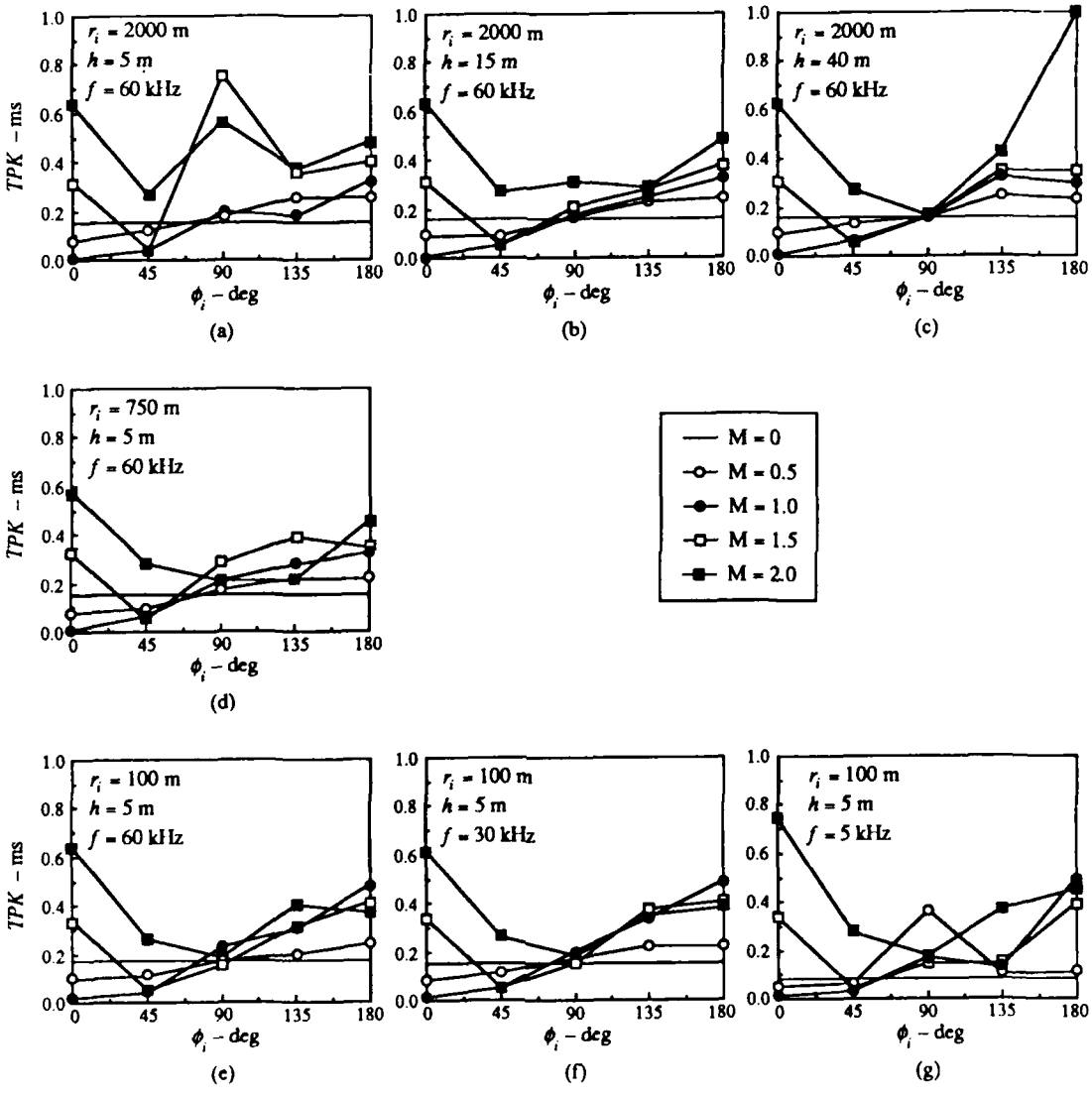

Figure 8 3 Time of Peak Pressure

ARL:UT
AS 87-324
LJG-GA
4-3-87

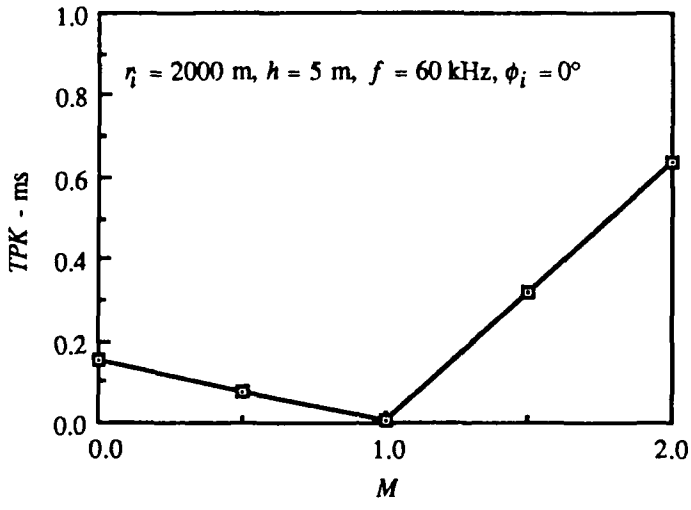

Figure 8-4 TIME of PEAK PRESSURE versus MACH NUMBER

Fig. 8-3 to be roughly symmetric about $M = 1$. However, a second effect resulting from inversion of the signal when $M > 1$ skews the curve. In our simulated signals from a stationary source, the peak pressure occurs relatively early. If the source is moved rapidly, so that the entire source line appears to the receiver to be moving with $M > 1$, then the signal is inverted. This has the effect of delaying the time after signal onset at which the peak pressure is observed. From Fig. 8-4 we conclude that the time inversion is more important above $M = 1$ than the time straining.

The cases used to generate Figs. 8-3(a)-(c) are identical except for the depth of the receiver. On comparing these figures it can be concluded that TPK is sensitive to changes in h, and more so when the velocity of the laser on the surface of the water, v, is greater than the speed of sound in water, c. However, note that TPK is not sensitive to changes in h when $M = 0$.

Figures 8-3(a), (d), and (e) were generated from identical situations except for the source-to-receiver range. Except when $M = 0$, TPK is sensitive to changes in r_0, and more so when $v > c$. Note that varying either r_0 or h has the effect of changing the apparent source speed. Hence it is not surprising that the pattern of signal variations is similar in the two cases.

Figures 8-3(e)-(g) represent identical cases except for the modulation frequency of the laser. They show that TPK is sensitive to changes in f, even when $M = 0$. The fact that the frequency of modulation affects TPK even for a stationary source is primarily a low frequency effect. At very high modulation frequencies, one would expect that the laser intensity envelope peak would determine the sound peak time regardless of the modulation.

From these results we conclude that the time of the peak pressure is sensitive to changes in ϕ_0, M, h, f, and r_0.

8–1.3 TIME INVERSION PROPERTY, TPK/TD

For our laser, the peak amplitude of the laser intensity occurs relatively early. Therefore, the ratio TPK/TD can be used as a measure of the degree of time inversion of the received acoustic signal. However, it is important to note that for different laser intensity profiles TPK/TD may not be a measure of time inversion. For example, in a symmetric pulse with the peak occurring exactly at the midpoint of the pulse, TPK/TD would remain constant at a value of 0.5 regardless of the degree of time inversion.

Since time inversion of the signal can only occur if the source is moving, no time inversion takes place if $M = 0$. Therefore the ratio of TPK/TD for $M = 0$ can be used as a reference for measuring the level of time inversion of the received signal. Figure 8-5 shows the results for TPK/TD. By comparing Figs. 8-5(a)-(g) one sees that TPK/TD is generally not sensitive to changes in ϕ_0 when $v < c$, but is quite sensitive to changes in ϕ_0 when $v \geq c$ and the laser is moving towards the receiver. Also, note that TPK/TD is generally not sensitive to changes in M when the laser is moving away from the receiver, but is sensitive to changes in M when the laser is moving towards the receiver, especially as M goes from 0.5 to 1.5. In other words, the received signal is heavily time inverted when the laser velocity is greater than the sound speed, and is moving towards the receiver. Furthermore, the level of time inversion is highly dependent on ϕ_0 and M.

Figures 8-5(a)-(c) were generated from identical cases except for the depth of the receiver. They show that TPK/TD is fairly insensitive to changes in h as these changes only affect RM in a minor way.

The cases used to generate Figs. 8-5(c)-(g) are exactly the same except for the modulation frequency of the laser. These figures show that TPK/TD

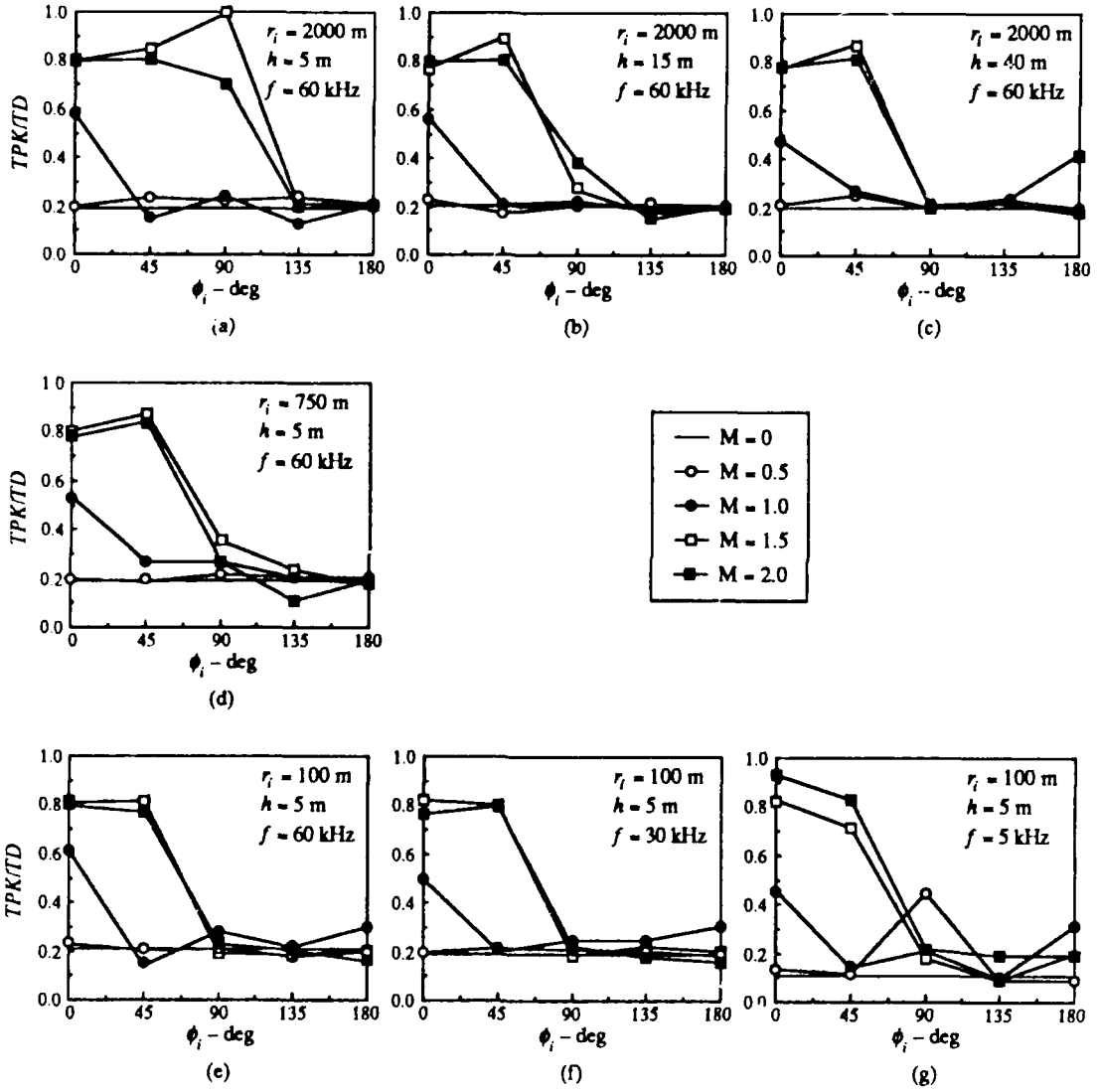

Figure 8-5 Time Inversion Property

AD-A192 220 AN ANALYSIS OF THE EFFICIENCY AND DIRECTIVITY OF THE SOUND GENERATED BY A (U) TEXAS UNIV AT AUSTIN APPLIED RESEARCH LABS R J CHANDRASEKHAR ET AL 13 AUG 87 2/2

UNCLASSIFIED ARL-TR-87-42 N00014-85-K-0819 F/G 20/1 NL

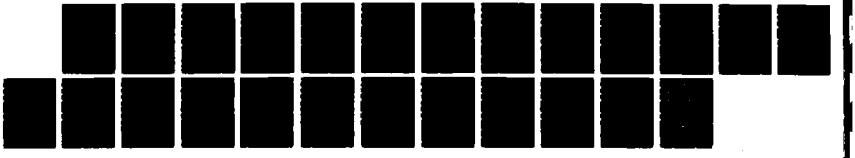

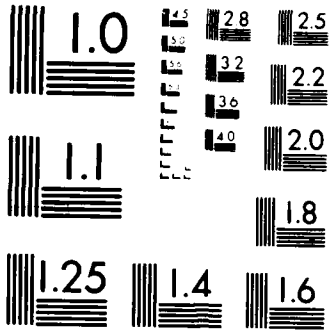
1.0
1.1
1.25
1.4
1.6
1.8
2.0
2.2
2.5
2.8
3.2
3.6
4.0

is fairly insensitive to changes in f. As in the case of TPK, any variation in TPK/TD would be expected to be a low frequency affect associated with delays in the peak of the laser intensity due to modulation.

Figures 8-5(a), (d), and (e) were generated from identical situations except for the source-to-receiver range. They show that TPK/TD is also fairly insensitive to changes in r_0.

From these results we conclude that the time property TPK/TD is primarily sensitive to changes in ϕ_0 and M, so long as $M > 1$. Therefore the level of time inversion of the signal is very sensitive to changes in ϕ_0 and M.

8-1.4 MINIMUM PERIOD, *TMIN*

Figure 8-6 shows the results for $TMIN$, the minimum period in the received signal. Figures 8-6(a)-(g) show that $TMIN$ is quite sensitive to changes in ϕ_0 and M. However, notice that $TMIN$ is not sensitive to changes in ϕ_0 when the laser is stationary. Also, notice that when $\phi_0 = 90°$, $TMIN$ is the same regardless of the velocity of the laser. The latter result stems from the fact that, when $\phi_0 = 90°$, the Mach number as seen by the receiver is initially equal to zero and only increases slightly. Therefore the signal almost appears to be generated by a stationary source. Nevertheless, one would expect $TMIN$ to increase slightly as M increases from 0 to 2 at $\phi_0 = 90°$, since the signal will be slightly stretched in time when the laser is moving away from the receiver; the data in which results were printed up to the fourth significant digit do not show this. It is most likely that the difference was simply too small to detect.

Figures 8-6(a)-(g) show that $TMIN$ is particularly sensitive to changes in the velocity of the laser when it is moving directly towards and away from the receiver, that is, when ϕ_0 equals 0° and 180°, respectively. These figures also

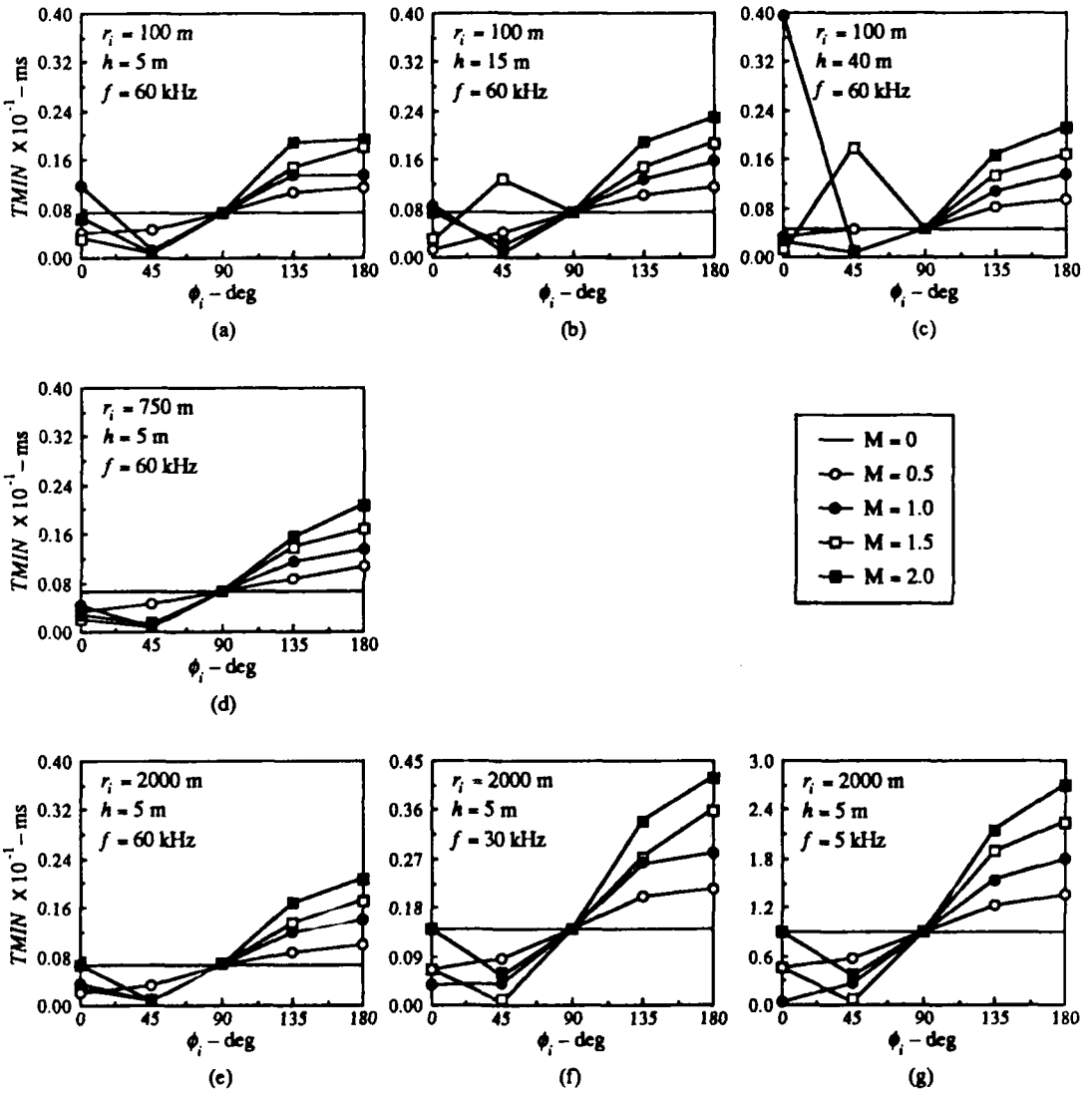

Figure 8-6 MINIMUM PERIOD

ARL:UT
AS-87-326
LJG-GA
4-3-87

show that $TMIN$ increases monotonically (with respect to M) when the laser is moving away from the receiver. The largest value of $TMIN$ in all cases occurs when $\phi_0 = 180°$ and $M = 2$. As discussed earlier, this case produces the greatest stretching of the received signal, and therefore the largest $TMIN$.

Figures 8-6(a)-(c) were generated from identical cases except for the depth of the receiver. They show that $TMIN$ is sensitive to changes in h, particularly when the source is moving towards the receiver, and M equals 1 or 1.5.

The cases used to generate Figs. 8-6(e)-(f) are identical except for the modulation frequency of the laser. As would be expected, these figures show that $TMIN$ decreases as the frequency increases. Also, the data for these cases indicate that $TMIN$ acts almost as if it were inversely proportional to f, regardless of the Mach number.

Figures 8-6(a), (d), and (e) represent identical situations except for the source-to-receiver range. These figures show that $TMIN$ is not particularly sensitive to changes in r_0.

From these results we conclude that the time property $TMIN$ is sensitive to changes in h, f, M, and ϕ_0. In addition, the manner in which $TMIN$ varies with respect to f, M, and ϕ_0 is quite evident.

8-1.5 MAXIMUM PERIOD, $TMAX$

Figure 8-7 shows the results for $TMAX$, the maximum period in the received signal. Figures 8-7(a)-(g) show that $TMAX$ is very sensitive to changes in ϕ_0 and M. As for the previous properties, $TMAX$ is not sensitive to changes in ϕ_0 when the laser is stationary. All the graphs in Fig. 8-7 indicate that $TMAX$ is least sensitive to changes in M when $\phi_0 = 90°$. Again, for this case the Mach number as seen by the receiver is nearly equal to zero for the duration of the pulse;

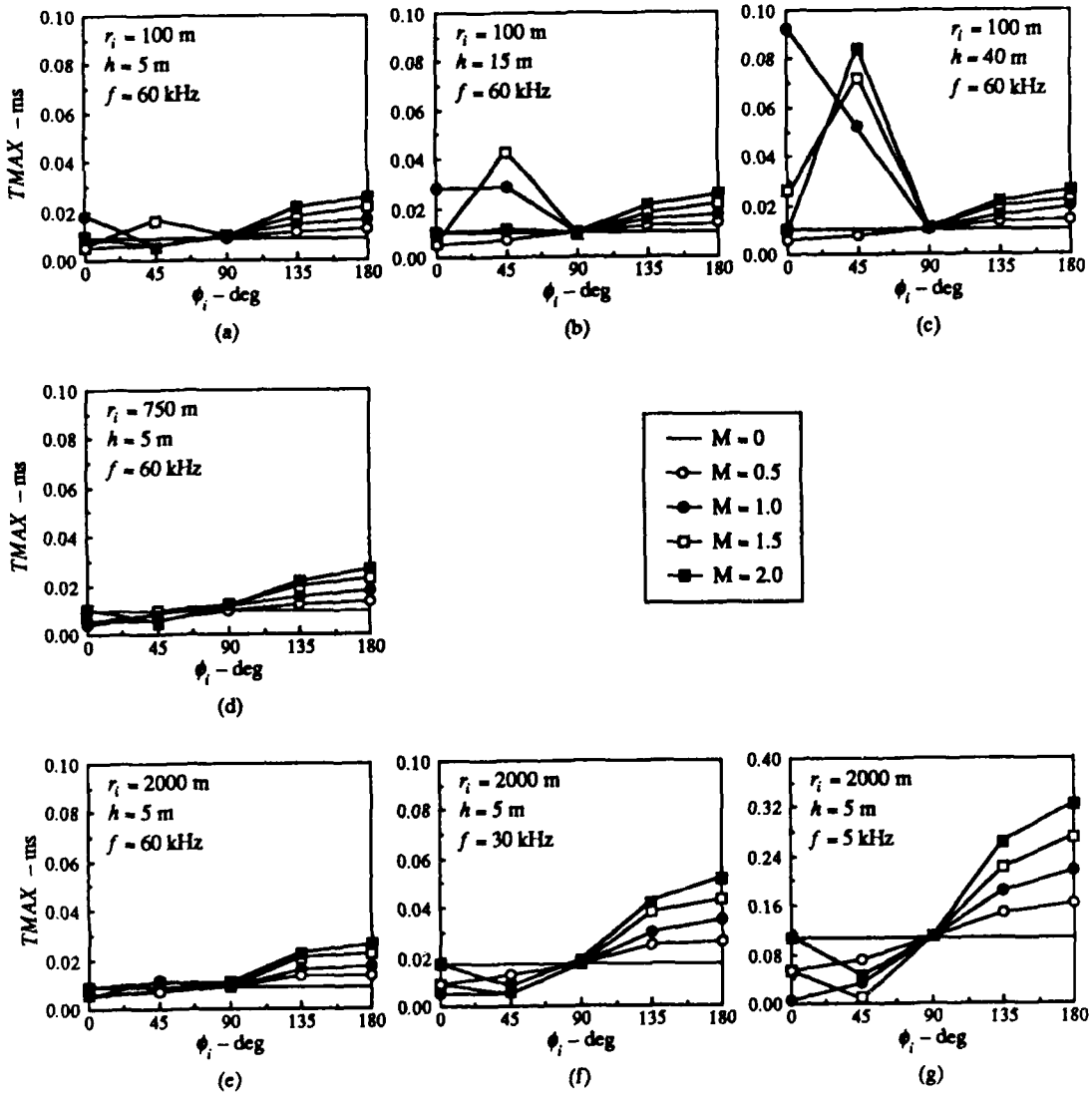

Figure 8-7 MAXIMUM PERIOD

therefore the sound appears to be generated by an almost stationary source. However, the data for these cases do show that $TMAX$ generally increases slightly as the velocity of the laser increases. Like $TMIN$, $TMAX$ increases monotonically (with respect to M) when the laser is moving away from the receiver. The largest value of $TMAX$ in all cases occurs when $\phi_0 = 180°$ and $M = 2$, since this combination induces the greatest stretching of the received signal.

Figures 8-7(a)-(c) represent identical cases except for the depth of the receiver. They show that $TMAX$ is sensitive to changes in h, and especially when $v \geq c$.

The cases used to generate Figs. 8-7(e)-(g) are identical except for the modulation frequency of the laser. Like $TMIN$, $TMAX$ decreases as the frequency increases, and also acts almost as if it were inversely proportional to f.

Figures 8-7(a), (d), and (e) were generated by identical situations except for the source-to-receiver range. These figures show that $TMAX$ is not particularly sensitive to changes in r_0.

From these results we conclude that the time property $TMAX$ is sensitive to changes in the parameters h, f, M, and ϕ_0. Also, like $TMIN$, the manner in which $TMAX$ varies with respect to f, M, and ϕ_0 is very evident.

8-1.6 AVERAGE PERIOD, $TAVE$

Figure 8-8 shows the results for $TAVE$, the average of all periods in the received signal. Like the two previous time properties, $TAVE$ is very sensitive to changes in ϕ_0 and M. Also, $TAVE$ is least sensitive to changes in M when $\phi_0 = 90°$, but the data for these cases indicate that $TAVE$ increases slightly as M increases. Like $TMIN$ and $TMAX$, $TAVE$ increases monotonically (with respect to M) when the laser is moving away from the receiver. In all cases, the

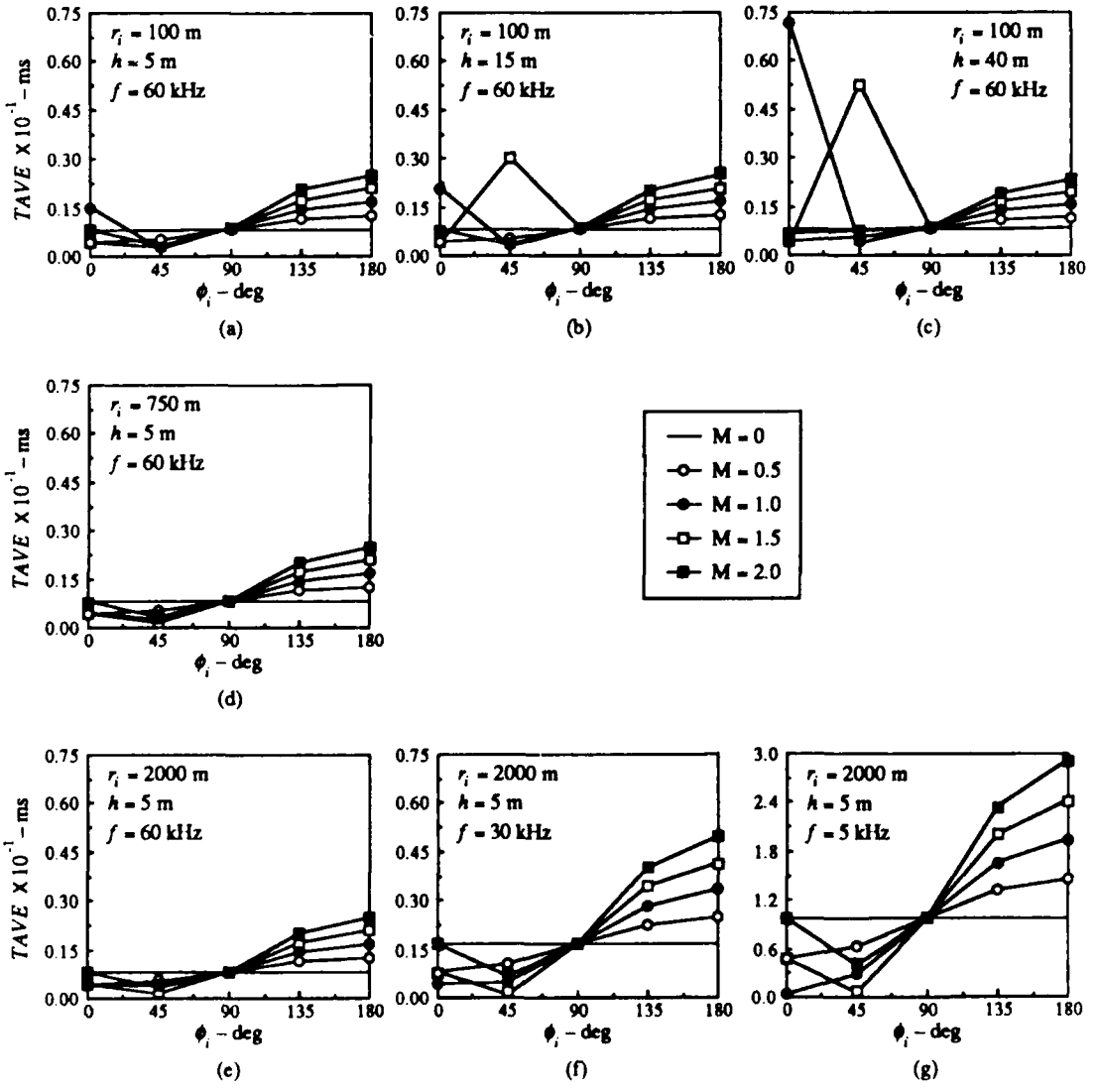

Figure 8-8 Average Period

largest value of $TAVE$ occurs when $\phi_0 = 180°$ and $M = 2$, since this combination of parameters induces the greatest elongation of the received signal.

Figures 8-8(a)-(c) were generated from identical cases except for the depth of the receiver. These figures show that $TAVE$ is sensitive to h, particularly when M equals 1 or 1.5, and the source is moving towards the receiver.

The cases used to generate Figs. 8-8(e)-(g) are identical except for the modulation frequency of the laser. Like $TMIN$ and $TMAX$, $TAVE$ decreases as the modulation frequency increases, and also behaves almost as if it were inversely proportional to f.

Figures 8-8(a), (d), and (e) represent identical situations except for the source-to-receiver range. These figures show that $TAVE$ is not very sensitive to changes in r_0.

From these results we conclude that $TAVE$ is sensitive to changes in the parameters h, f, M, and ϕ_0, and that its behavior, like $TMIN$ and $TMAX$, with respect to changes in f, M, and ϕ_0 is very evident.

8-2 PRESSURE RELATED PROPERTIES

The pressure related properties are those which are acquired from the pressure peak or the root mean square pressure: PPK, $PRMS$, and $PPK/PRMS$.

8-2.1 PRESSURE PEAK, PPK, AND ROOT MEAN SQUARE PRESSURE, $PRMS$

Figure 8-9 shows the results for PPK, the absolute peak pressure of the received signal. Figures 8-9(a)-(g) show that PPK is very sensitive to changes in ϕ_0 and M. However, notice that PPK is not sensitive to changes in ϕ_0 when the laser is stationary. Also, PPK is least sensitive to changes in M when $\phi_0 = 90°$.

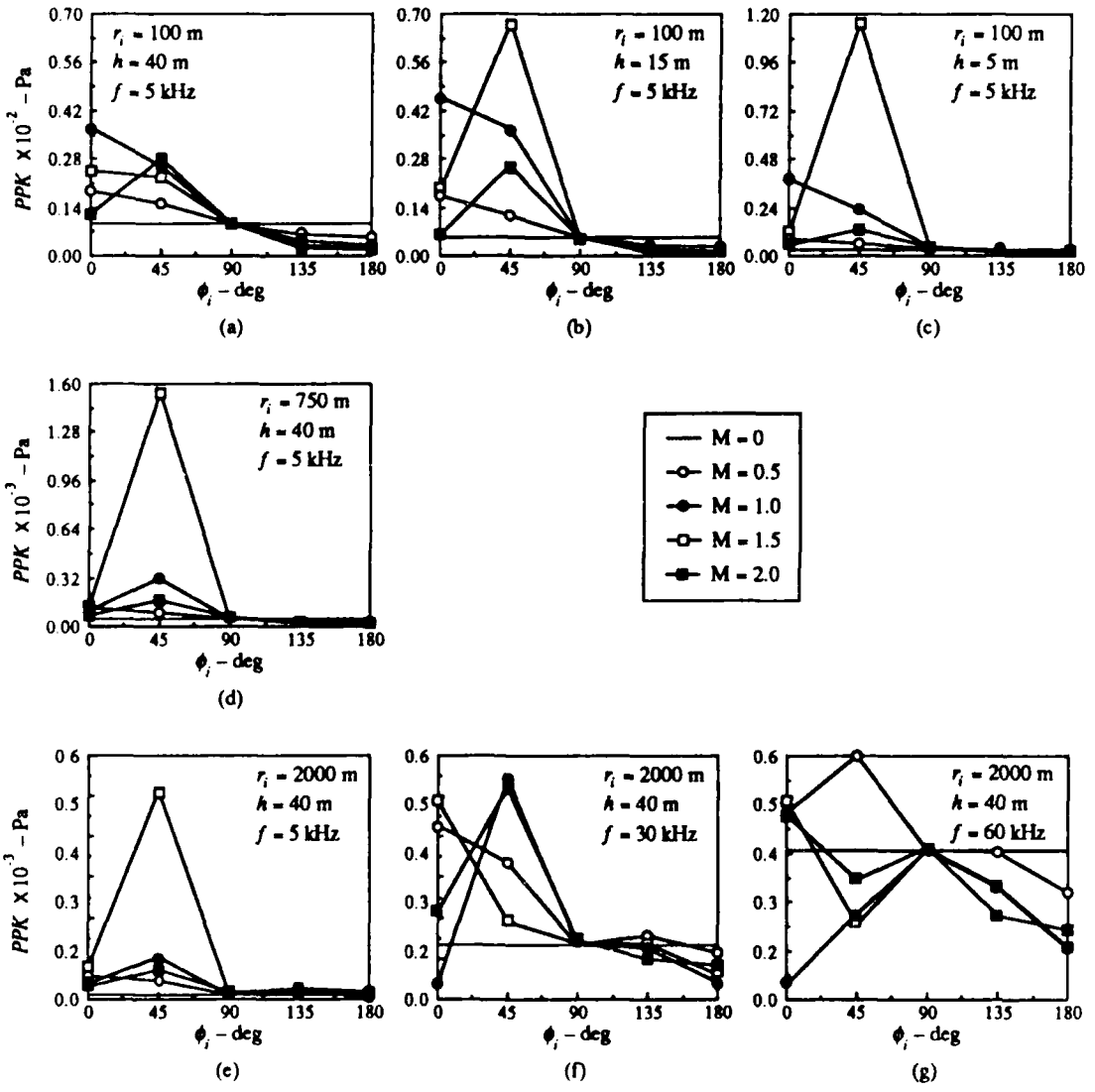

Figure 8 9 Pressure Peak

since at this point the sound initially appears to be generated by a stationary source. Figures 8–9(a)–(g) also show that PPK is less sensitive to changes in M when the laser is moving away from the receiver, and that generally PPK decreases under these conditions as M increases.

Figures 8–9(a)–(c) represent identical cases except for the depth of the receiver. From these three graphs one sees that PPK generally increases as h increases when M equals 0.5 or 2, and decreases with increasing h when M equals 1 or 1.5.

The cases used to generate Figs. 8–9(e)–(g) are identical except for the modulation frequency of the laser. These figures show that PPK generally increases as f increases. This result can be explained by the fact that the magnitude of the time derivative of the laser intensity (which drives the pressure) increases as f increases.

Figures 8–9(a), (d), and (e) were generated from identical situations except for the source-to-receiver range. These figures show that PPK generally decreases as r_0 increases due to spherical spreading.

From these results we conclude that the absolute peak pressure is sensitive to changes in all of the parameters.

The results for $PRMS$ are shown in Fig. 8–10. The patterns of behavior as parameters are varied are identical for $PRMS$ and PPK. Hence we conclude that $PRMS$ is sensitive to changes in all the parameters.

8–2.2 PRESSURE RATIO, $PPK/PRMS$

The results for $PPK/PRMS$ are shown in Fig. 8–11. Figures 8–11(a)–(g) show that $PPK/PRMS$ is quite sensitive to changes in c_0 and M. Like all of the previous properties, $PPK/PRMS$ is not sensitive to changes in the angle

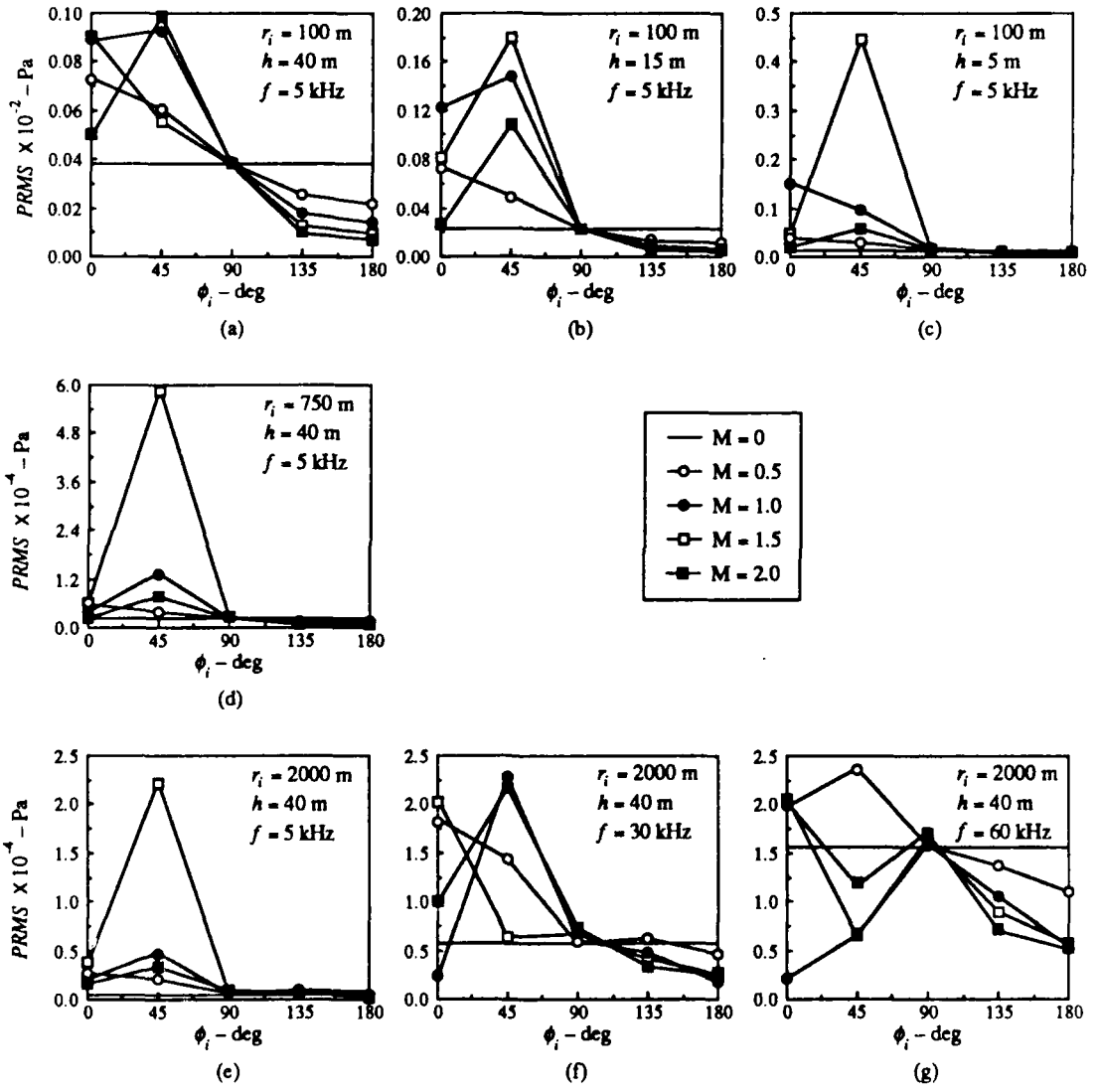

Figure 8-10 Root Mean Square Pressure

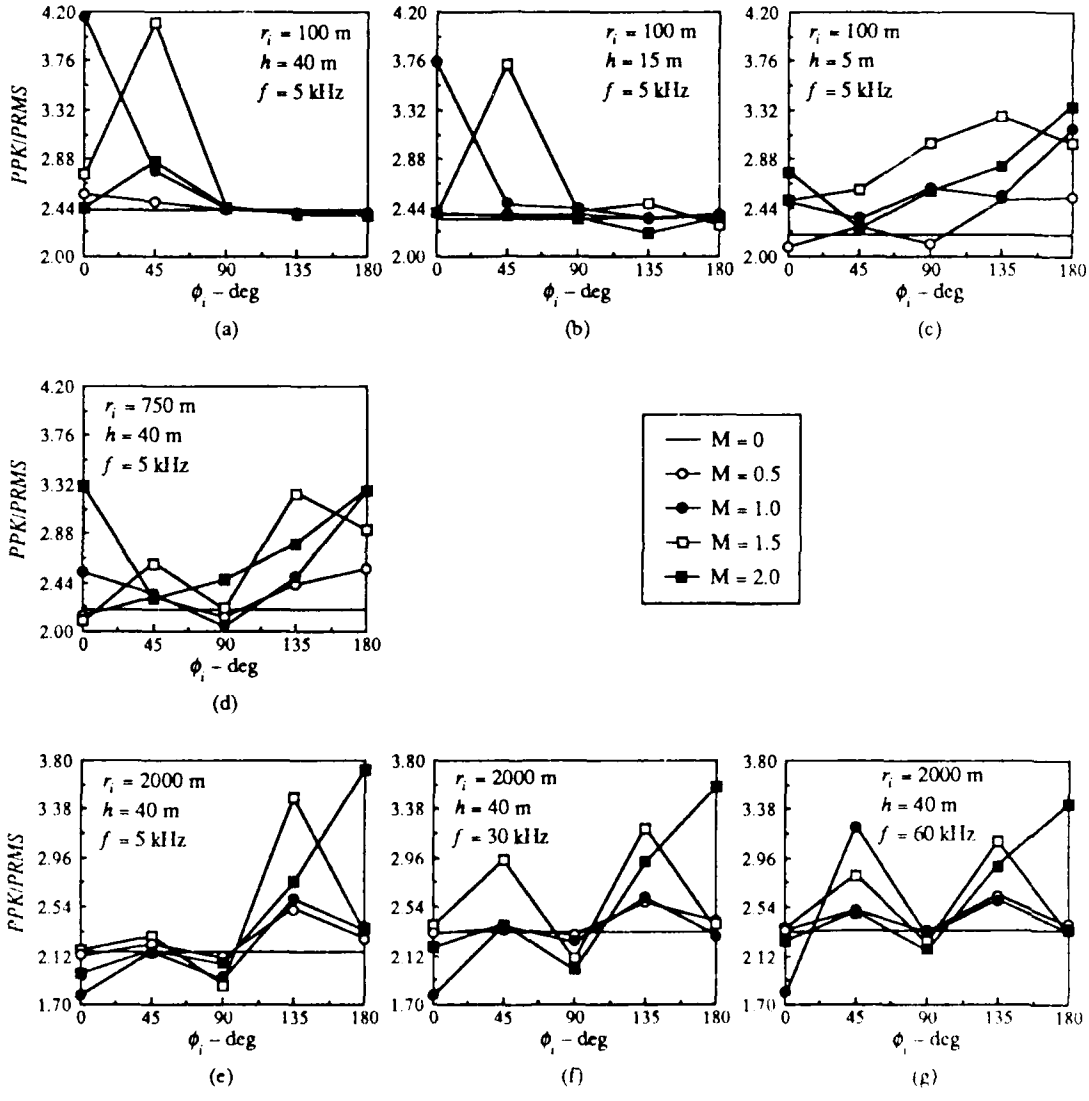

Figure 8 11 PRESSURE RATIO

ϕ_0 when the laser is stationary. Also, notice that $PPK/PRMS$ is sensitive to changes in M even when $\phi_0 = 90°$.

Figures 8-11(a)-(c) represent identical cases except for the depth of the receiver. From these three graphs one sees that $PPK/PRMS$ is very sensitive to changes in h, but that its sensitivity to changes in h decreases as h increases.

The cases used to generate Figs. 8-11(e)-(g) are identical except for the modulation frequency of the laser. These figures show that $PPK/PRMS$ is quite sensitive to changes in f. In particular, $PPK/PRMS$ seems to be more sensitive to changes in f when the laser is moving towards the receiver.

Figures 8-11(a), (d), and (e) were generated from identical situations except for the source-to-receiver range. They show that $PPK/PRMS$ is very sensitive to changes in r_0.

From these results we conclude that the ratio $PPK/PRMS$ is sensitive to changes in all the parameters. In fact, it is the most sensitive measure studied.

CHAPTER 9

SUMMARY AND CONCLUSIONS

This part of the report has discussed a numerical investigation of the generation of underwater sound by a moving high power laser source. The acoustic signal generated by the moving laser was studied in detail. Properties of the signal were identified and the manner in which these properties change with respect to source and receiver parameters was quantified. This information identified the aspects of the sound signal that are least and most susceptible to change.

A computer program called MTS, written by Berthelot,[19] with modifications suitable for this project, was used to numerically predict the received acoustic signal. This computer program is based on the time domain approach discussed in Chapter 1.

The parameters of the source which were varied were the modulation frequency, f, of the laser intensity and the velocity, v, or Mach number, $M = v/c$, of the laser beam on the surface of the water. The source-receiver geometrical parameters which were varied were the initial distance between the source and receiver, r_0, the initial horizontal angle, ϕ_0, and the depth of the receiver, h. The values of the parameters were carefully chosen to cover the whole range of physically realizable situations. All possible combinations of the parameters were used, resulting in a total of 675 cases.

The properties of the received acoustic signal which were examined may be placed into two categories: time related and pressure related properties. The time related properties of the acoustic signal which were numerically investigated were the duration of the received signal TD, the time at which the absolute peak pressure occurs TPK, the maximum period in the signal $TMAX$, the minimum period $TMIN$, the average of all periods $TAVE$, and the time inversion property TPK/TD. The pressure related properties studied were the absolute peak pressure PPK, the root mean square pressure of the acoustic signal $PRMS$, and the pressure ratio $PPK/PRMS$.

The results showed that TD is very sensitive to changes in the initial horizontal angle, ϕ_0, and the Mach number, M, of the laser beam on the surface of the water. However, TD is not sensitive to changes in the angle ϕ_0 when the source is stationary. Also, TD is least sensitive to changes in M when $\phi_0 = 90°$. In the case when $\phi_0 = 90°$, the Mach number as seen by the receiver, RM, is initially equal to zero, and remains approximately equal to zero for the duration of the laser pulse. To the receiver, then, the sound essentially appears to be generated by a stationary source. Hence the duration of the received pulse is relatively constant.

It was also found that TD increases monotonically (with respect to M) as the laser moves away from the receiver. The maximum duration of the received signal occurs when the laser is moving directly away from the receiver. The results also showed that TD is most sensitive to changes in M when the laser is moving directly towards the receiver, or directly away from the receiver. However, the results showed that TD is very insensitive to changes in the parameters r_0, f, and h.

From these results it was concluded that TD is dependent on the apparent

speed of the source. In terms of geometrical parameters, this means that the duration of the received signal is highly dependent on ϕ_0 and M.

Like the time property TD, the results showed that TPK is quite sensitive to changes in ϕ_0 and M. For a stationary source, TPK, like TD, is not a function of ϕ_0. When the laser is moving directly towards the receiver, the results showed that TPK decreases as RM goes from 0 to 1, and increases as RM goes from 1 to 2. This is a result of the signal being compressed in time, as $RM = 1$ is approached from below and above. It was found that TPK is not symmetric about $RM = 1$. A second effect, resulting from inversion of the signal when $RM > 1$, skews the curve.

The results also showed that TPK is sensitive to changes in h, especially when the velocity of the laser on the surface of the water is greater than the speed of sound in water. It was also found that TPK is sensitive to changes in f, even when $M = 0$. Except when $M = 0$, TPK is sensitive to changes in r_0, and more so when $v > c$. From these results it was concluded that TPK is sensitive to changes in all the parameters.

The results showed that the time inversion property, TPK/TD, is generally not sensitive to changes in ϕ_0 when $v < c$, but is quite sensitive to changes in ϕ_0 when $v \geq c$, and the laser is moving towards the receiver. Also, TPK/TD is generally not sensitive to changes in M when the laser is moving away from the receiver, but is sensitive to changes in M when the laser is moving towards the receiver. The results also showed that TPK/TD is fairly insensitive to changes in h, f, and r_0. From these results it was concluded that the received signal is heavily time inverted when the laser velocity is greater than the sound speed, and is moving towards the receiver. In addition, the level of time inversion is highly dependent on ϕ_0 and M.

The property $TMIN$ was found to be quite sensitive to changes in ϕ_0 and M. However, $TMIN$ is not sensitive to changes in ϕ_0 when the laser is stationary. Also, no change in $TMIN$ was detected as M was varied when $\phi_0 = 90°$. Again, for this case the signal appears to be generated by an almost stationary source. The results also showed that $TMIN$ is particularly sensitive to changes in the velocity of the laser when it is moving directly towards and away from the receiver.

It was also found that $TMIN$ increases monotonically (with respect to M) when the laser is moving away from the receiver. The largest value of $TMIN$ occurs when the laser is moving directly away from the receiver, since this condition produces the greatest stretching of the received signal.

The results showed that $TMIN$ is sensitive to changes in h, particularly when the source is moving towards the receiver, and M equals 1 or 1.5. As expected, $TMIN$ was found to act almost as if it were inversely proportional to f, regardless of the Mach number. The results also showed that $TMIN$ is not particularly sensitive to changes in r_0.

The patterns of behavior as parameters were varied for $TMAX$ and $TAVE$ were found to be practically identical to those of $TMIN$. The only difference in their behavior was found to occur when $\phi_0 = 90°$. When $\phi_0 = 90°$, both $TMAX$ and $TAVE$ were found to increase slightly as M was increased.

From these results, it was concluded that $TMAX$ and $TAVE$ are sensitive to changes in the parameters h, f, M, and ϕ_0. Furthermore, the manner in which $TMAX$ and $TAVE$ vary with respect to f, M, and ϕ_0 is very evident.

The numerical results showed that PPK is very sensitive to changes in ϕ_0. However, PPK was found to be insensitive to changes in ϕ_0 when the laser is stationary, since at this point the sound initially appears to be generated by a stationary source. Also, PPK is less sensitive to changes in M when the laser is

moving away from the receiver, and generally decreases under these conditions.

The results also showed that PPK generally increases as h increases and as f increases. The latter can be explained by the fact that the magnitude of the time derivative of the laser intensity (which drives the pressure) increases as f increases. Furthermore, the results showed that PPK generally decreases as r_0 increases. This decrease is due to spherical spreading. From these results it was concluded that PPK is sensitive to changes in all of the parameters.

The results for $PRMS$ showed that its patterns of behavior as parameters are varied are identical to those of PPK. It was concluded that $PRMS$ is sensitive to changes in all the parameters.

Finally, the results showed that $PPK/PRMS$ is very sensitive to changes in ϕ_0 and M. Like all of the previous properties, $PPK/PRMS$ is not sensitive to changes in the angle ϕ_0 when the laser is stationary. Also, $PPK/PRMS$ was found to be sensitive to changes in M even when $\phi_0 = 90°$. The results also showed that $PPK/PRMS$ is very sensitive to changes in h and r_0. Furthermore, it was found that $PPK/PRMS$ is quite sensitive to changes in f, especially when the laser is moving towards the receiver. From these results it was concluded that the ratio $PPK/PRMS$ is sensitive to changes in all the parameters, and that this measure is more sensitive than any other studied.

Taken as a whole, this numerical study has shown that ϕ_0 and M are the most critical parameters, affecting virtually all of the received signal properties. In addition, f is a critical parameter for all of the pressure related properties, and the time related properties derived from the zero crossing of the received signal. Hence, if thermoacoustic generation of sound is to be used for communication, extreme care must be taken that M, ϕ_0, and f are well known.

REFERENCES

[1] L. M. Lyamshev and L. V. Sedov, "Optical generation of sound in a liquid: thermal mechanism (review)," *Sov. Phys.-Acoust.* **27** (1), 4-18 (1981).

[2] L. M. Lyamshev and K. A. Naugol'nykh, "Optical generation of sound: nonlinear effects (review)," *Sov. Phys.-Acoust.* **27** (5), 357-371 (1981).

[3] U. Ingard, "Acoustics," *Handbook of Physics* (McGraw-Hill, New York, 1953).

[4] P. J. Westervelt and R. S. Larson, "Laser-excited broadside array," *J. Acoust. Soc. Am.* **54**, 121-122 (1973).

[5] T. G. Muir, C. R. Culbertson, and J. R. Clynch, "Experiments on thermoacoustic arrays with laser excitation," *J. Acoust. Soc. Am.* **59**, 735-743 (1976).

[6] F. V. Bunkin, A. I. Malyararovskii, V. G. Mikhalevich, and G. P. Shipulo, "Experimental investigation of the acoustic field of a moving optoacoustic antenna," *Sov. J. Quantum Electon.* **8**, 270-271 (1978).

[7] F. V. Bunkin, A. I. Malyarovskii, and V. G. Mikhalevich, "Experimental study of pulsed sound fields excited by moving laser thermooptical sources," *Sov. Phys.-Acoust.* **27**, 98-102 (1981).

[8] A. I. Bozhkov, F. V. Bunkin, I. B. Esipov, A. I. Malyorivskii, and V. G. Makhalevich, "Moving laser thermooptical sources of ultrasound," *Sov. Phys.-Acoust.* **26**, 100-104 (1980).

[9] L. M. Lyamshev and L. V. Sedov, "Generation of sound by a moving pulsed optoacoustic source," *Sov. Phys.-Acoust.* **25**, 510-514 (1981).

[10] Y. H. Berthelot and I. J. Busch-Vishniac, "Laser-induced thermoacoustic radiation," *J. Acoust. Soc. Am.* **78**, 2074–2082 (1985).

[11] Y. H. Berthelot and I. J. Busch-Vishniac, "Thermoacoustic radiation of underwater sound by a moving high-power laser source," *J. Acoust. Soc. Am.* Suppl. 1, **77**, S103 (1985).

[12] Y. H. Berthelot and I. J. Busch-Vishniac, "Thermoacoustic radiation of sound by a moving laser source," *J. Acoust. Soc. Am.* **81**, 317–327 (1987).

[13] R. S. Larson, "Optoacoustic interactions in fluids," Applied Research Laboratories Technical Report No. 74-21 (ARL-TR-74-21), Applied Research Laboratories, The University of Texas at Austin (1974).

[14] V. S. Gorodetskii, S. V. Egerev, I. B. Esipov, and K. A. Naugol'nykh, "Generation of sound by laser pulses," *Sov. J. Quantum Electron.* **8** (11), 1345–1347 (1978).

[15] L. V. Burmistrova, A. A. Karabutov, O. V. Rudenko, and E. B. Cherepetskaya, "Influence of thermal nonlinearity on the thermooptical generation of sound," *Sov. Phys.–Acoust.* **25** (4), 348–350 (1979).

[16] T. A. Lunina, S. V. Egerev, L. M. Lyamshev, and K. A. Naugol'nykh, "Nonlinear theory of the thermal mechanism of sound generation by a laser," *Sov. Phys.–Acoust.* **25** (4), 353–354 (1979).

[17] H. A. Hsieh, "Design of laser-induced-heating configurations for generation and control of underwater sound beams," Ph.D. thesis, Georgia Institute of Technology, Atlanta, Georgia, March 1987.

[18] A. D. Pierce and H. A. Hsieh, "Achievement of substantially higher source levels for airborne-laser-induced underwater sound," *J. Acoust. Soc. Am.* Suppl. 1, **77**, S104 (1985).

[19] Y. H. Berthelot, "Generation of underwater sound by a moving high-power laser source," Applied Research Laboratories Technical Report No. 85-21 (ARL-TR-85-21), Applied Research Laboratories, The University of Texas at Austin (1985).

[20] A. D. Pierce, "Energy partitioning and optical to acoustic conversion efficiency during laser generation of underwater sound," *J. Acoust. Soc. Am.* Suppl. 1, **74**, S78 (1983).

[21] A. D. Pierce and Y. H. Berthelot, "Validity of linear acoustics for prediction of waveforms caused by sonically moving laser beams," submitted to *J. Acoust. Soc. Am.*, June 1987.

[22] C. R. Culbertson, N. P. Chotiros, and Y. H. Berthelot, "Experimental apparatus for studying moving thermoacoustic sources," Applied Research Laboratories Technical Report No. 83-24 (ARL-TR-83-24), Applied Research Laboratories, The University of Texas at Austin (1983).

13 August 1987

DISTRIBUTION LIST FOR
ARL-TR-87-42
FINAL REPORT UNDER CONTRACT N00014-85-K-0819

Copy No.	
1	Chief of Naval Research Office of Naval Research Department of the Navy Arlington, VA 22219 Attn: R. Fitzgerald (Code 1125UA)
2 - 7	Director Naval Research Laboratory Washington, D.C. 20375 Attn: Library
8	Commander Space and Naval Warfare Systems Command Washington, D.C. 20363-5101 Attn: CAPT L. Wardle (Code PDW-106-6)
9	Commander David Taylor Naval Ship Research and Development Center Target Physics Branch Bethesda, MD 20084 Attn: S. Schreppler (Code 1965)
10	Superintendent Naval Postgraduate School Department of Physics Monterey, CA 93940 Attn: Steve Garrett
11-22	Commanding Officer and Director Defense Technical Information Center Bldg. 5, Cameron Station 5010 Duke St. Alexandria, VA 22314

Distribution List for ARL-TR-87-42 under Contract N00014-85-K-0819 (cont'd)

Copy No.

School of Mechanical Engineering
Georgia Technical Institute
Atlanta, GA 30332
23 Attn: Yves Berthelot
24 Allan Pierce
25 Jacek Jaarzynski

National Center for Physical Acoustics
University of Mississippi
University, MS 38677
26 Attn: Larry Crum
27 Hank Bass

Department of Physics
Kalamazoo College
Kalamazoo, MI 49007
28 Attn: Wayne Wright

Department of Engineering
Yale University
Mason Laboratory
9 Mill House Ave.
New Haven, CT 06520
29 Attn: Bob Apfel

Mechanical Engineering Department
The University of Texas at Austin
Austin, TX 78712
30 Attn: Mark Hamilton
31 Dennis Wilson
32 Deborah Summa
33 Erland Veffring

Electrical Engineering Department
The University of Texas at Austin
Austin, TX 78712
34 Attn: Elmer Hixson

Institute of Sound and Vibration Research
The University
Southampton S09 5NH
ENGLAND
35 Attn: Chris Morfey

Distribution List for ARL-TR-87-42 under Contract N00014-85-K-0819
(cont'd)

Copy No.	
	Physics Department Lawrence Livermore National Lab L-298 P.O. Box 808 Livermore, CA 94550
36	Attn: Stephen I. Warshaw
	Federal Bureau of Investigation Engineering Section 8199 Backlick Rd. Lorton, VA 22079
37	Attn: Stanley Rodak
38	Richard Brown
39	David T. Blackstock, ARL:UT
40	Charles E. Bradley, ARL:UT
41	Ilene Busch-Vishniac, ARL:UT
42	Nicholas P. Chotiros, ARL:UT
43	Frederick D. Cotaras, ARL:UT
44	C. Robert Culbertson, ARL:UT
45	Dean J. Driebe, ARL:UT
46	Thomas A. Griffy, ARL:UT
47	James A. Hawkins, ARL:UT8
48	Stephen J. Lind, ARL:UT
49	James A. TenCate, ARL:UT
50	Evan K. Westwood, ARL:UT
51	Library, ARL:UT

END

DATE

FILMED

6-88

DTIC